Formation, Ageing and Thermal Properties of Secondary Organic Aerosol

Eva Emanuelsson

Ph.D. thesis
Department of Chemistry and Molecular Biology
University of Gothenburg

Faculty of Science

UNIVERSITY OF GOTHENBURG

THESIS FOR THE DEGREE OF DOCTOR OF PHILOSOPHY IN CHEMISTRY

Formation, ageing and thermal properties of secondary organic aerosol

Eva Emanuelsson

UNIVERSITY OF GOTHENBURG

FACULTY OF SCIENCE

DOCTORAL THESIS
UNIVERSITY OF GOTHENBURG
DEPARTMENT OF CHEMISTRY AND MOLECULAR BIOLOGY
GOTHENBURG, SWEDEN 2013

Formation, ageing and thermal properties of secondary organic aerosol

Eva Emanuelsson

Department of Chemistry and Molecular Biology
University of Gothenburg
SE-412 96 Göteborg, Sweden

ISBN 978-91-628-8620-2
E-publication: http://hdl.handle.net/2077/31839

Photo on cover: BSOA(?) at Femstenaberg, Skee 2007

Printed by Ale Tryckteam AB

#362 *Jävla Svin* Ordfront Galago 2011

Abstract

In order to properly represent and predict the effects of aerosol in climate systems, an accurate description of their formation and properties is needed. This thesis describes work done to increase the knowledge of processes and properties of atmospherically relevant secondary organic aerosol (SOA) from both biogenic and anthropogenic origin. The common theme for these projects is the use of a Volatility Tandem Differential Mobility Analyser (VTDMA) setup, which in combination with other observations has generated insight into both detailed chemical mechanisms and physical processes that eventually could be suitable for testing in air quality or climate models. During the course of this work, the experimental facility the Gothenburg Flow Reactor for Oxidation Studies at low Temperatures (G-FROST) and the VTDMA setup, as well as a corresponding data evaluation methodology, have been improved and refined.

Thermal properties could be linked to both formation and ageing processes of SOA. Using a VTDMA setup, where the thermal characteristics of SOA were measured at a range of evaporation temperatures, a sigmoidal fit to the data enabled parameterisation of their volatility properties. The parameters extracted were e.g. the temperature corresponding to a volume fraction remaining of 0.5 ($T_{VFR0.5}$) and the slope factor (S_{VFR}), which are measures of the general volatility and the volatility distribution of the condensed phase products, respectively. A higher $T_{VFR0.5}$ indicates lower volatility, while an increase of S_{VFR} states a broader distribution of vapour pressures. The response of these parameters from changes in experimental conditions could be linked to processes occurring both in the gaseous and the condensed phase. In photo-chemical experiments, the change in $T_{VFR0.5}$ and S_{VFR} could be described using the OH dose.

The gas phase processes were found to be very important for SOA ageing, driven mainly by OH radical exposure in the outdoor chamber SAPHIR. However, processes in the condensed phase, such as plausible non oxidative ageing processes and non-liquid behaviour of SOA particles, were also observed.

Detailed studies of ozonolysis of the boreal forest monoterpenes β-pinene and limonene were enabled by precise control of reaction conditions using the G-FROST. The experimental findings in response to e.g. water and radical conditions emphasized the difference in ozonolysis reaction paths between endo- and exocyclic compounds. The results support the recently suggested decomposition of the stabilized Criegee Intermediate via the hydroperoxide channel in ozonolysis of β-pinene.

Keywords

volatile organic compounds, biogenic, anthropogenic, secondary organic aerosol, troposphere, volatility, ozone

Populärvetenskaplig sammanfattning

Luften omkring oss innehåller inte bara gaser, utan också små partiklar. Dessa partiklar varierar i storlek från nano- till mikrometer och påverkar livet på jorden på många sätt. De är bland annat viktiga för jordens energibalans. För att förutspå framtida klimat används idag datormodeller för att uppskatta den solenergi som når jorden och hur stor del som reflekteras mot rymden. En viktig del i modellerna är effekten av moln och partiklar i luften, som kräver kunskap om från vad och hur de bildas, åldras och försvinner.

Partiklarna kan ha naturligt ursprung eller komma från mänsklig aktivitet. En grupp av partiklar bildas från nedbrytning av organiska molekyler i gas. Den tydliga doften av skog eller en gammal bil på tomgång är exempel på dessa ämnen. I nedbrytningsmekanismerna är solljus och marknära ozon viktiga komponenter. Marknära ozon skapas när bilavgaser eller föroreningar från annan förbränning utsätts för solljus. Ozonet reagerar sedan med bland annat organiska molekyler i luften. Idag är det bara en bråkdel av alla ämnen i atmosfären kända. I den kemiska cocktail som bildas är det svårt att följa alla reaktioner som skapar nya molekyler, som sedan reagerar med varandra i ett komplicerat nätverk av reaktioner.

Hur atmosfäriska partiklar bildas och åldras kans studeras i olika typer av försökskammare. Där kan olika processer ske under kontrollerande betingelser och partiklarnas bildning och egenskaper mätas med olika typer av instrument. En viktig del av forskningen om atmosfären innebär att utveckla kammare, analysinstrument och metoder för att utvärdera mätresultaten.

Arbetet inom denna doktorsavhandling har experimentellt studerat bildning och åldrande av partiklar som uppstått ur kombinationer av organiska ämnen i luften omkring oss. Från dessa data har parametrar tagits fram som beskriver partiklarnas egenskaper och sammansättning, som också kan länkas till åldringsprocesser av partiklar från solljus. Även nedbrytningsmekanismen mellan ozon och organiska ämnen från växtlighet har studerats. Denna kunskap kan användas för att förbättra beskrivningen av partiklarnas effekter i klimatmodeller.

Popular scientific summary

The air around us is not only gases, but also small particles. These particles in the size from nano- to micro meter affects life on Earth in several ways. They are among other things important for the energy balance of the Earth. To predict future climate, computer models are used to estimate the energy from the sun that reach Earth or is reflected into space. One important part of the models is the description of the effect from clouds and particles in the air, which requires knowledge of their formation, ageing and disappearance.

Particles can have both biologic and man-made origin. One group of particles is formed from degradation of gaseous organic compounds. The distinct scent of a forest, or an old car on idle are examples of these organic compounds. In the degradation mechanisms are sunlight and ground level ozone are important components. Ground level ozone is formed when automobile emissions or air pollutants from other combustion are exposed to sunlight. The ozone then can react with organic compounds present in air. Today only a minority of all organic compounds in the atmosphere are known. In the chemical cocktail in the atmosphere it is difficult to follow the reactions generating new compounds, which then reacts in a more complex network of reactions.

The formation and ageing of atmospheric particles can be studies in several types of experimental chambers, where the formation and properties of the particles in controlled conditions can be measured by different types of instruments. An important part of atmospheric research implicates development of chambers, instruments for analysis and data evaluation methods.

The work within the doctoral thesis has experimentally studied the formation and ageing of particles from combinations of organic compounds in ambient air. From this data parameters that describe the properties and composition of the particles have been developed, which also can be linked to ageing processes of particles from sunlight. Also the ozone degradation mechanism of organic compounds from vegetation has been studied. These findings can be used to improve the part from particles in climate models.

List of Papers

Paper I

Influence of humidity, temperature and radicals on the formation and thermal properties of Secondary Organic Aerosol (SOA) from ozonolysis of β-pinene

E. U. Emanuelsson, Å. K. Watne, A. Lutz, E. Ljungström, and M. Hallquist
Submitted to *Journal of Physical Chemistry*

Paper II

Influence of Ozone and Radical Chemistry on Limonene Organic Aerosol Production and Thermal Characteristics

R. K. Pathak, K. Salo, E. U. Emanuelsson, C. Cai, A. Lutz, Å. M. Hallquist, and M. Hallquist
Environmental Science & Technology, 2012, 46, 11660−11669
dx.doi.org/10.1021/es301750r
Reprinted by permission from *Environmental Science & Technology*

Paper III

Formation of anthropogenic secondary organic aerosol (SOA) and its influence on biogenic SOA properties

E. U. Emanuelsson, M. Hallquist, K. Kristensen, M. Glasius, B. Bohn, H. Fuchs, B. Kammer, A. Kiendler-Scharr, S. Nehr, F. Rubach, R. Tillmann, A. Wahner, H.-C. Wu, and Th. F. Mentel
Atmospheric Chemistry and Physics Discussions, 2012, 12, 20311–20350.
doi:10.5194/acpd-12-20311-2012

Paper IV

Formation, ageing and thermal properties of secondary organic aerosol from photo-oxidation of selected boreal terpene mixtures

E. U. Emanuelsson, C. Spindler, B. Bohn, T. Brauers, H. -P. Dorn, R. Häseler, F. Rubach, R. Tillmann, A. Kiendler-Scharr, E. Schuster, H. Pleijel, Å. M. Hallquist, Th. F. Mentel and M. Hallquist
Manuscript

List of Abbreviations

ABL	Atmospheric Boundary Layer
ABSOA	Anthropogenic Biogenic Secondary Organic Aerosol
AMS	Aerosol Mass Spectrometer
ASOA	Anthropogenic Secondary Organic Aerosol
AVOC	Anthropogenic Volatile Organic Compound
BMT	Boreal Mono Terpene
BSOA	Biogenic Secondary Organic Aerosol
BVOC	Biogenic Volatile Organic Compound
CCN	Cloud Condensation Nuclei
CI*	Criegee Intermediate (excited)
CPC	Condensation Particle Counter
DMA	Differential Mobility Analyser
Ea	Activation energy
FZJ	Forschungszentrum Jülich
GC-FID	Gas Chromatography Flame Ionisation Detector
GC-MS	Gas Chromatography Mass Spectrometry
G-FROST	Gothenburg Flow Reactor for Oxidation Studies at low Temperatures
IPCC	Intergovernmental Panel on Climate Change
IVOC	Intermediate Volatile Organic Compound
JPAC	Jülich Plant Atmosphere Chamber
K	Kelvin
LIF	Laser Induced Fluorescence
LVOC	Low Volatile Organic Compound
m/z	Mass to charge ratio
MFC	Mass Flow Controller
MT	Mono Terpene
Mw	Molecular weight
NMDp	Normalised Modal Diameter
NMVOC	Non Methane Volatile Organic Compound
NVOC	Non Volatile Organic Compound
OH	Hydroxyl radical
O/C	Oxygen to Carbon ratio
$\overline{OS}$	Average carbon oxidation state

PAN	Peroxy Acetyl Nitrate
PC	Plant Chamber
PID	Proportional Integral Derivative
PM_1, $PM_{2.5}$, PM_{10}	Mass of particles with an aerodynamic diameter less than 1, 2.5, 10 µm respectively
POZ	Primary Ozonide
ppb	parts per billion (American billion i.e. 10^9)
ppt	parts per trillion
PTR-MS	Proton Transfer Mass Spectrometry
P-ToF	Particle Time of Flight
QAMS	Quadrupole Aerosol Mass Spectrometer
RC	Reaction Chamber
RH	Relative Humidity
S	Saturation ratio
SAPHIR	Simulation of Atmospheric PHoto chemistry In a large Reaction chamber
SCI	Stabilized Criegee Intermediate
SLMP	Standard Litre Per Minute
SMEAR	Station for Measuring Forest Ecosystem Atmosphere Relations
SMPS	Scanning Mobility Particle Sizer
S_{VFR}	Slope factor
SVOC	Semi Volatile Organic Compound
SOZ	Secondary Ozonide
SOA	Secondary Organic Aerosol
TD	Thermo Denuder
$T_{VFR0.5}$	Temperature corresponding to VFR=0.5
UV	Ultra Violet
VBS	Volatility Basis Set
VFR	Volume Fraction Remaining
VFR_{TD}	Volume Fraction Remaining Thermo Denuder
VOC	Volatile Organic Compound
VTDMA	Volatility Tandem Differential Mobility Analyser

Contents

1 Introduction

1.1 Formation, ageing and thermal properties of secondary organic aerosol

1.1.1 Do aerosol particles matter?

The ambient air is essential for life. Each cubic centimetre contains thousands of liquid or solid particles. The size ranges from nanometres to several tens of micrometres in diameter. By definition, *an aerosol is a mixture of solid or liquid particles suspended in a gaseous medium* (Hinds, 1999). Thus we are surrounded and affected by aerosol in various ways and aspects in our daily life. The impacts of aerosol are as diverse as beautifully coloured sunsets, respiratory drug distribution, disintegration of cultural-historical statues and buildings, the complex taste of champagne, or the Sisyphean work of keeping the windows clean.

Atmospheric science includes several sub disciplines such as meteorology, climatology, environmental science, biology, physics and chemistry. Joakim Pirinen's chubby young boy in the school desk asks:

> *Fysik och kemi, är inte det samma sak?*
> *Physics and chemistry, aren´t they the same thing?*

When the chemist from a molecular perspective focuses on how chemical compounds interact with each other and with energy (e.g. heat or radiation), the physicist is occupied with the fundamental principles of physical phenomena on a wider scale. To study and improve the knowledge on the formation, properties and impact of atmospheric aerosol, the long running collaborations between chemists and physicists have been and are most applicable. Another relevant area in this context is biology. Atmospheric science is indeed a trans-disciplinary field. The non-natural sciences, e.g. international law and socio economics applied on infrastructure and urbanization contribute important aspects to atmospheric science.

1.2 Focus of this thesis

The atmosphere is, together with the biosphere, lithosphere, hydrosphere and cryosphere, an integral part of the Earth's system. Tellus was a research platform at the University of Gothenburg, Faculty of Science, dedicated to Earth system science. Doctoral students and researchers from Earth sciences, biology and chemistry collaborated in order to gain a deeper understanding of the complex processes and interactions on Earth. The work presented in this thesis is one result of the efforts within Tellus to link the understanding of the atmosphere and the biosphere.

The scientific issues applicable to this thesis are the formation, ageing and thermal properties of Secondary Organic Aerosols (SOA) from both biogenic and anthropogenic precursors. Selected atmospherically relevant systems have been experimentally investigated with emphasis on volatility. The specific focus of this thesis is ozonolysis mechanism of monoterpenes, and other processes involved in both formation and ageing of secondary organic aerosol. The relationships obtained are aimed for use in atmospheric models. The experimental setup of the flow reactor G-FROST has been improved, and a new evaluation approach for volatility data has been developed. Several measurement campaigns have been conducted using the outdoor chamber SAPHIR, as well as emissions from a real boreal forest plant microcosm in the semi-flow/static plant chamber JPAC at the Forschungszentrum Jülich, Germany.

1.2.1 Outline of thesis

The first part of this thesis describes the background and puts the work into a wider context. The applications and the theoretical background of the concepts are described, as well as the experimental setups, and the basic design of the experiments. Then, the experimental data are evaluated, and put into a scientific perspective and discussed with regard to the objectives of this work. Finally, major conclusions are presented.

So far, the work within this project has resulted in four scientific papers, appended as Paper I-IV.

2 Background

2.1 Earth´s atmosphere

2.1.1 Gases

Everyone can relate to the atmosphere. The air we breathe, the sun, the wind and the rain. Earth's atmosphere is a gaseous cocktail with the main ingredients of nitrogen (N_2 78.08 %) and oxygen (O_2 20.90 %), with a splash of argon (Ar 0.93 %). The remaining 0.09 % is the numerous other gases present in small quantities, called trace gases. Examples are ozone (O_3), carbon dioxide (CO_2), nitrogen oxides (NO_x), sulphur dioxide (SO_2), ammonia, (NH_3), methane (CH_4), and volatile organic compounds (VOC). Despite their minute concentrations, the trace gases are important on both local and global scales as pollutants, greenhouse gases etc. Also water vapour is essential in the atmosphere, and varies from almost zero to 4 % depending on local metrological conditions.

The Earth's atmosphere is the thin layer of gas surrounding the Earth. Compared to the radius of Earth (6378 km at the equator), the atmosphere is a thin shell of approximately 80 km above ground. If Earth was the size of an apple, the atmosphere would be thinner than the peel of the apple. The atmospheric pressure at sea level is about 1013 hPa, decreasing approximately exponentially with height, dropping to half at an altitude of about 5.6 km.

The troposphere is reaching from the surface up to about 10 km at the poles and 15 km at the equator. Here is where essentially all of the water vapour, clouds and precipitation are found. The temperature decreases with increasing height until the tropopause, the region separating the troposphere from the stratosphere. This is where the temperature profile changes and the temperature starts to increase with height, caused by a critical series of photochemical reactions involving ozone and molecular oxygen responsible for generating a steady-state concentration of ozone, at approximately 25 km altitude. The stratospheric ozone, often referred to as the ozone layer, is essential for life on Earth because ozone strongly absorbs light with a wavelength, $\lambda < 290$ nm.

The properties of the Earth´s atmosphere have several aspects. One is the greenhouse effect, i.e. the heat insulating property that keeps the Earth's surface warm. The greenhouse effect results in an average surface temperature of approx. 14°C, compared to -19°C (254 K) if the atmosphere would have been transparent to thermal radiation (Hari and Kulmala, 2008). The bulk molecules and atoms of the atmosphere do not significantly interact with thermal radiation, but several of the trace gases do, the so

called greenhouse gases. They effectively absorb the outgoing thermal radiation emitted by the Earth's surface, and emit themselves the radiation in all directions. The major greenhouse gases are water vapour, carbon dioxide and ozone (Finlayson-Pitts and Pitts, 2000). Anthropogenic contributions are dominated by carbon dioxide, methane and ozone, see Figure 6. Water is important for the energy balance of the Earth also through its condensed phases, generating clouds, which absorb, reflect and emit radiation to varying degrees. The combined effects of aerosol are estimated to lead to a net cooling of the Earth, and thus offset part of the effect from greenhouse gases (IPCC, 2007).

Concentration of gases can be expressed as molecules per volume, which is most applicable when it comes to e.g. rate constants of chemical reactions, or mass per volume. Trace gases are typically given as a mixing ratio e.g. parts per American billion (ppb, 10^{-9}), which is the ratio of trace gas mole or volume to total mole or volume of air. It is notable, however, that mixing ratio is a dimensionless quantity, not a concentration. Each cubic centimetre air contains 2.46×10^{19} gas molecules (T=298 K, P=1013 hPa).

2.1.2 Mixing within the troposphere

The troposphere is often vertically well mixed, and the temperature is generally decreasing with an average rate of 6.5 K for every 1 km increase in height (lapse rate). This is caused mainly by adiabatic cooling of air, when an air parcel moves upward and pressure decreases. Warm air has lower density due to thermal expansion, and is thus moved upward, while colder air is denser and is descending. In addition, the water vapour content also affects the air density, as an air parcel with high water content has lower density than dry air at the same temperature and pressure. This causes strong vertical mixing to the tropopause in days or less, depending on the meteorological conditions.

The lowest part of the troposphere directly influenced by the presence of Earth´s surface is the atmospheric boundary layer (ABL). Here, in general the vertical mixing is strong, responding to surface forcing such as heating or cooling with a time scale of an hour or less. The capping inversion layer is the stably stratified layer that limits exchange between the ABL and the free troposphere above, and where the influence of the wind direction from the surface is negligible. The typical daytime boundary layer height during winter in Gothenburg is around 1 km (Olofson et al., 2009).

A typical daytime evolution of the atmospheric boundary layer in high pressure conditions over land is illustrated in Figure 1. After sunrise, the solar heating causes thermal plumes to rise, transporting moisture, heat and aerosol. The plumes rise and expand adiabatically until a thermodynamic equilibrium is reached at the top of the atmospheric boundary layer. The moisture transferred by the thermal plumes forms convective clouds. Dryer air penetrates down, replacing the rising air parcels, and the convective air motions generate intense turbulent mixing forming a mixed layer, where temperature and humidity are nearly constant with height. The height of the mixed layer can vary from a few hundred meters during the early morning development stage up to 2–3 km in mid-afternoon.

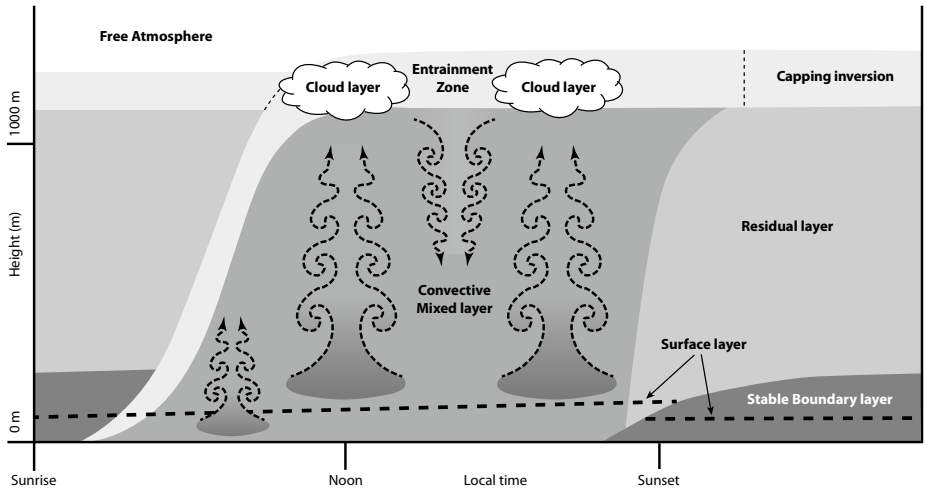

Figure 1: Schematic of the atmospheric boundary layer (ABL) diurnal development during high pressure conditions over land. Figure adapted from Stull, 1988.

The lowest part of the ABL is called the surface layer. In windy conditions, the surface layer is characterized by a strong, approximately logarithmic wind shear, caused by friction. Stability strongly affects the wind profile. In addition, in the vicinity of rough surfaces such as forests, a roughness sub layer exists where wind gradient is reduced. The thickness of the roughness sub layer is between one to two characteristic heights of the rough surface. Referring to forests, this is the forest height. Friction velocity is a good estimate for air mixing and boundary layer height. The smaller the friction velocity, the smaller the boundary layer height and vice versa.

The boundary layer from sunset to sunrise is called the nocturnal boundary layer. It is often characterized by a stable layer, which forms when the solar heating ends and the radiative cooling and surface friction stabilize the lowest part of the ABL. Above the surface layer, the remnants of the daytime convective layer forms a residual layer.

Under certain conditions, the normal vertical temperature gradient in the troposphere is inverted such that the air is colder near the surface of the Earth, i.e. a temperature inversion. An inversion suppresses convection by acting as a lid and can trap e.g. air pollution close to the ground. Subsidence inversions can occur when a warmer, less dense air mass moves over a cooler, denser air mass e.g. in the vicinity of warm fronts, and also in areas of oceanic upwelling such as along the Californian coast in the United States. In Gothenburg, strong ground inversions typically occur a few times per year during cold clear winter days.

2.2 Atmospheric aerosol particles

Physical particle size may properly be given by one parameter (e.g. diameter) only if the particle is spherical, e.g. a liquid droplet. Since particles often have irregular shape, it is common to give the equivalent aerodynamic diameter. This is the diameter d of a sphere of unit density that has the same settling velocity as the particle in question. Thus, d says more about the aerodynamic behaviour of the particle than about its actual, physical size. Most measurement instruments dealing with particle size relate to the equivalent aerodynamic diameter.

Aerosol particles can be divided into coarse and fine particles, with a saddle point at 1-3 μm (Hinds, 1999), see Figure 2. Typically, the larger coarse particles are mechanically generated, originating e.g. from sea spray, soil, road dust or plants. The fine particles have three characteristic modes below 1 μm; the nucleation, Aitken and accumulation modes.

Particles can be expressed as number or mass per unit volume. Small particles dominate the number concentration, while larger particles contribute mainly to mass (volume). Size distributions of both number (Figure 3) and mass (Figure 4) of atmospheric aerosol

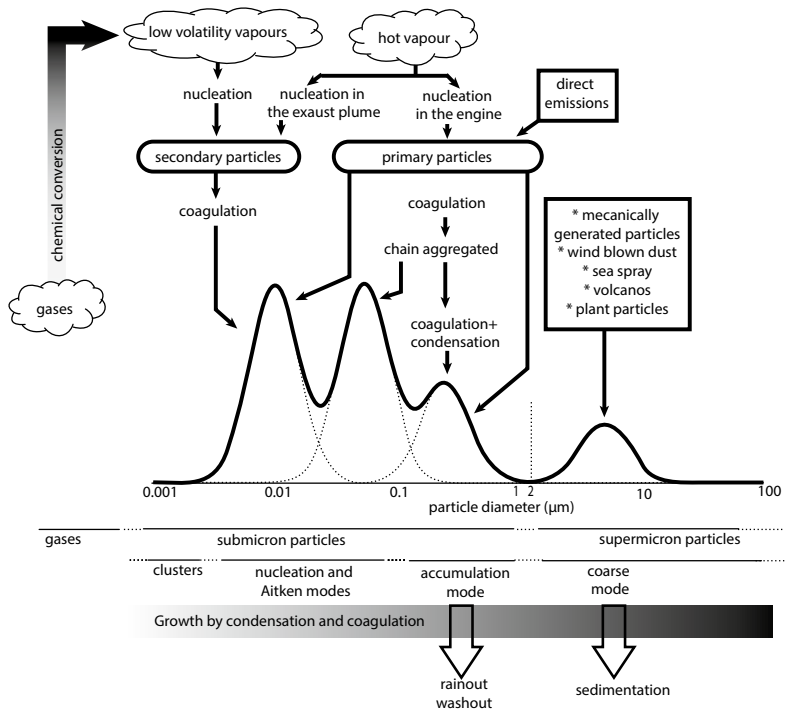

Figure 2: Overview of aerosol size classification together with main sources and sinks. Figure adapted from Whitby and Sverdrup, 1980.

particles differ in different environments, as aerosol sources, sinks and properties alter. Particles are typically collected using devices with a known aerodynamic diameter cut-off. PM_{10} refers to a mass of particles with a diameter below 10 µm, $PM_{2.5}$ below 2.5 µm and PM_1 below 1 µm.

Once emitted or formed in the atmosphere, particles can grow by vapour condensation or by coagulation with other particles. Small particles may diffuse to surfaces or serve as nucleation sites for raindrops (rainout). Larger particles are removed by settling or impaction on surfaces such as tree leaves, or by falling rain or snow (washout).

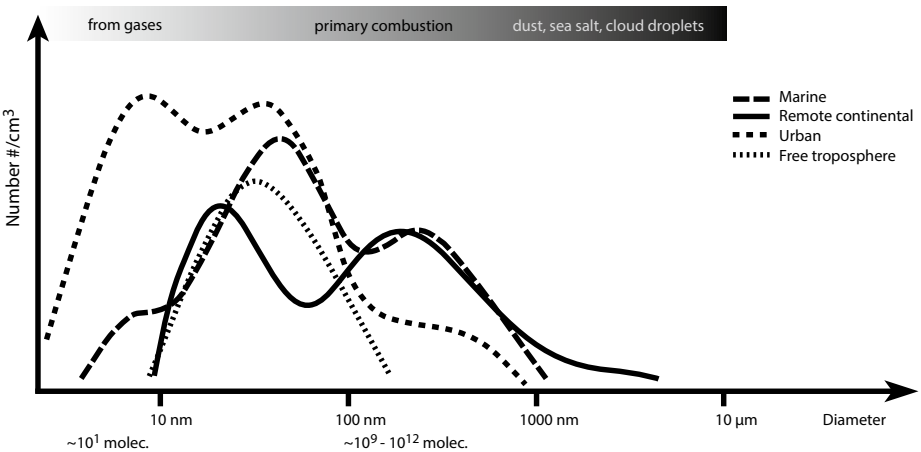

Figure 3: Size distributions of atmospheric aerosol particles in different environments. Figure adapted from H. Vehkamäki and V.-M. Kerminen.

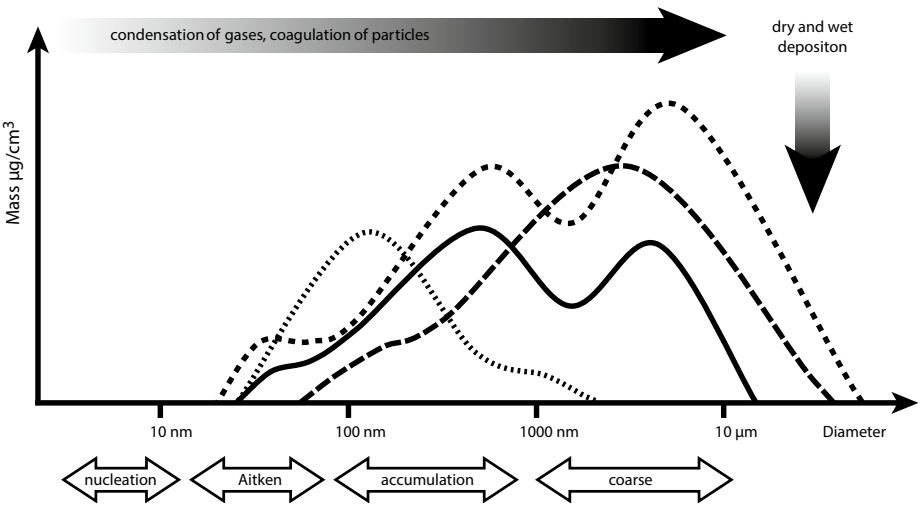

Figure 4: Mass distributions of atmospheric aerosol particles in different environments. Figure adapted from H. Vehkamäki and V.-M. Kerminen.

Particles in the accumulation mode have lifetimes of days in the troposphere, while larger particles (d > 20 μm) are removed in a matter of hours (Hinds, 1999). Particles in the stratosphere, i.e. above the tropopause, may persist for long periods of time. Relatively little vertical mixing occurs in the stratosphere, and no precipitation scavenging occurs in this region. As a result, massive injections of particles, for example from volcanic eruptions such as the Mt. Pinatubo eruption in 1991, often produce long lasting particle layers.

2.2.1 Formation of secondary particles

Atmospheric aerosol particles can be divided into primary particles (emitted as particles) and secondary particles (from condensable vapours). The major components in the primary particles include soil-related material (e.g. Fe, Si, Ca, Mg), soot and organic matter (e.g. pollen and spores).

The secondary particles are formed by nucleation of gas molecules undergoing chemical processes, typically oxidation of organic molecules forming low vapour pressure products. The secondary organic aerosol (SOA) originates from volatile organic compounds (VOC), that can have either biogenic (biological) or anthropogenic (man-made) origin. The secondary particles contain e.g. nitrates, sulphates, oxygen and organic carbon.

Nucleation can be divided into two types, heterogeneous and homogenous. Heterogeneous nucleation occurs by condensation onto already pre-existing nuclei (e.g. ion clusters), while homogenous nucleation involves the formation of particles by intra molecular forces (e.g. van der Waal forces) present in all gases. Secondary organic aerosol is formed from gas phase reactions of organic precursor compounds, where the semi-volatile products undergo gas to particle conversion. The initial thermodynamics and kinetics of atmospheric aerosol particle formation and growth, i.e. the nucleation mechanism where gases initially form clusters and may end up as freshly formed nano-particles, are not yet fully understood. However, schematically the processes of secondary organic aerosol (SOA) formation and evolution can be described as in Figure 5.

$$\begin{array}{lcccccc} precursor_{gas} & \xrightarrow{i} & semi\text{-}volatile_{gas} & \xrightarrow{ii} & products_{gas} & & \rightarrow \\ & & \uparrow\downarrow & & \uparrow\downarrow & \downarrow\uparrow & \\ & & semi\text{-}volatile_{particle} & \xrightarrow{iii} & products_{particle} & & \rightarrow \end{array}$$

Figure 5: Schematic presentation of SOA formation and evolution mechanisms, showing multiple generations of gas-phase and particle-phase reactions.

Oxidation of the organic precursor in the gas phase (reaction i), forms semi-volatile products that partition between gas and particle. Then, the chemistry goes on generating new products in ether gas phase (reaction ii) or particle phase (reaction iii) that can partition between gas and particle. One significant part of the atmospheric aerosol is the semi-volatile compounds that are continuously transferred between gas and particle phase.

The degradation of gaseous volatile organic compounds in the atmosphere is initiated by reaction with hydroxyl (OH) or nitrate (NO_3) radicals, ozone (O_3) or by photolysis. In the marine atmosphere, chlorine atoms (Cl) may also initiate the oxidation of VOCs under certain conditions (Hallquist et al., 2009). The relative importance of these competing reactions varies depending on the structure of the organic compounds. The initial oxidation step forms a set of organic products containing one or more polar oxygenated functional groups, which typically make the products less volatile (less prone to exist in gas phase) and more water soluble. Examples are in falling order of contribution to volatility; ketone, aldehyde, alcohol and carboxylic acids (Pankow and Asher, 2008). The products generated by oxidation of VOCs are nucleating and/or condensing on to already existing particles.

2.2.2 Aerosol ageing

After the initial formation of particles, the aerosol undergoes both chemical and physical processes with time, often referred to as aerosol ageing. Further oxidation to form second generation products (and third, fourth and so on) may form products with even lower volatility and higher water solubility. Or the opposite, if the carbon chain is fragmented, forming smaller, often more volatile, compounds. Ageing through oxidation may take place both in gaseous and condensed phase. These reactions can be reflected as the oxygen content in the aerosol particle increase. A measure of the oxidative state of aerosol is often referred to as the ratio of strongly oxygenated fragment to less oxygenated fragments, from an aerosol mass spectrometer (AMS) instrument. But the ageing processes also include e.g. photolysis and oligomerisation, which not necessarily involves increased oxygen in the particle. Oxidations of organic compounds will ultimately generate water and the thermodynamically favoured CO_2.

2.3 Environmental effects of atmospheric particles

The impacts of atmospheric aerosol are diverse, but are normally divided into two main areas; climate and health. The SOA from biogenic precursors are considered of high interest for the effects on climate.

2.3.1 Particles and climate

The effect of aerosol on the temperature on Earth occurs through several different mechanisms, which can be divided into direct and indirect effects. The direct effects refer to the scattering, reflection and absorption of radiation by particles, or the deposition on snow/ice lowering the reflection coefficient (albedo), i.e. the reflecting power of Earth surface. The indirect effects are particles affecting e.g. cloud albedo and lifetime. The sum of each of these components, which separately can have a positive (warming) or negative (cooling) effect, determines the energy balance on Earth. This can be referred to as radiative forcing, *a measure of the influence a factor has in altering the balance of*

incoming and outgoing energy in the Earth-atmosphere system, and is an index of the importance of the factor as a potential climate change mechanism (IPCC, 2007).

A useful way of expressing the radiative forcing is provided in the latest IPCC report: *radiative forcing values are for changes relative to preindustrial conditions defined at 1750 and are expressed in watts per square meter (W m^{-2})* (IPCC, 2007). In this report (Figure 6), the total anthropogenic radiative forcing is estimated to 1.6 W m^{-2}, where the long lived greenhouse gases together contribute to 2.14 W m^{-2}. The overall influence of aerosol particles (total aerosol) is estimated to be negative, i.e. cooling of Earth, and thus offset some of the positive effects from the greenhouse gases. The effects of the greenhouse gases on the climate are quite well understood, but the overall influence of aerosol has high uncertainties. The cooling effect from total aerosol is estimated to -1.2 W m^{-2}, and is rated a low level of scientific understanding. The net effect of the direct effects from aerosol is estimated to give a negative radiation forcing, and the indirect effects due to clouds are also estimated negative (IPCC, 2007).

Most clouds are located in the troposphere. Clouds significantly affect the short-wave as well as the long-wave radiation field in the atmosphere and at the surface. Clouds increase the albedo of the Earth atmosphere system by scattering the solar radiation,

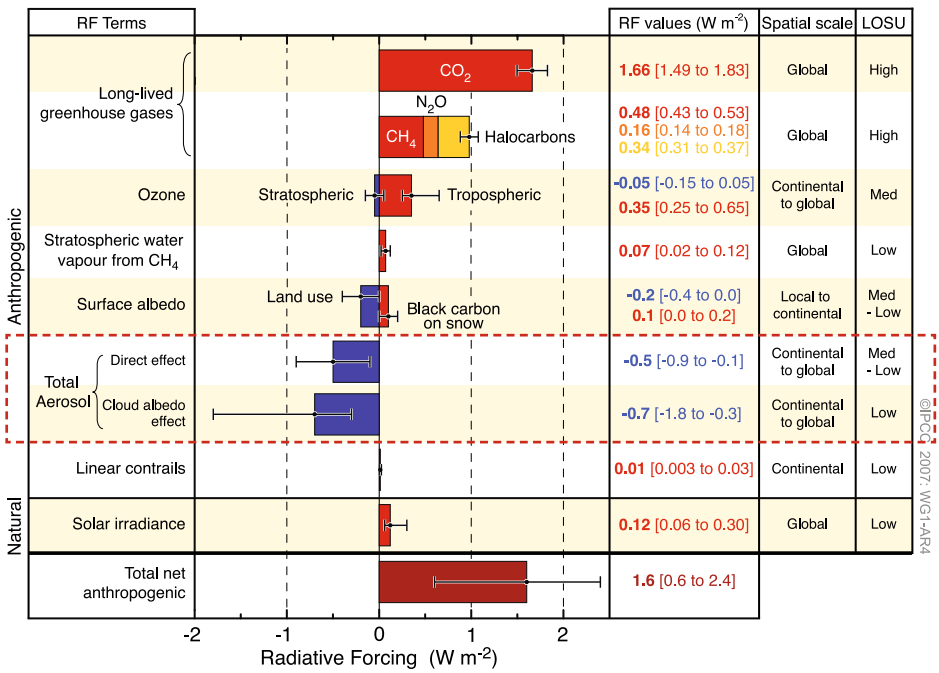

Figure 6: Estimated impact on average global atmospheric radiative forcing (RF) due to human influence for 2005. The corresponding level of scientific understanding (LOSU) is also indicated. Illustration from the IPCC fourth assessment report 2007 (WGI Figure SPM 2).

thus having a global average short-wave cooling effect of about 50 W m^{-2}. By reducing outgoing long-wave radiation by 30 W m^{-2}, clouds contribute to the greenhouse effect by about 20 W m^{-2} (Wielicki et al., 1995).

One important property of atmospheric aerosol particles is their capacity to act as cloud condensation nuclei (CCN), i.e. the core/surface where water can condense and form cloud droplets. This applies for atmospheric aerosol particles larger than 30-100 nm (Jimenez et al., 2009). An increasing number of aerosol particles increase the number of cloud droplets, while each droplet becomes smaller. This influences cloud properties, as the cloud becomes whiter and increases its albedo, and in addition, the lifetime of the cloud increases as precipitation is strongly dependent on droplet size.

Atmospheric nanometre sized particles affect Earth in as large scale as they are small (!). The energy balance of Earth should not be considered as a simple net of components with positive and negative contributions. Feedback mechanisms are likely to be important, both within and between the bars presented in Figure 6. They are not well understood, neither on a local nor on a global scale. The level of scientific understanding regarding aerosol is low, where the main question concerns the aerosol contributions to radiative forcing - mirror or blanket?

2.3.2 Particles and health

The respiratory system of a normal adult processes 10-25 m^3 (12-30 kg) of air per day. The upper part of the human respiratory system efficiently removes coarse particles, while smaller particles reach deeper. Nano sized particles can pass into the blood stream through the respiratory system (Heal et al., 2012). The possibility to relatively easy access the body through the airways has made aerosol particles a tool for the administration of medicinal drugs.

Particle size, surface area and chemical composition determine the health risk. Outdoor and indoor air quality is an issue in both industrialised and developing countries. The concern over air pollution on human health can be traced back many centuries, and traditionally mainly respiratory diseases (e.g. silicosis and asbestosis), have been considered. Today also cardio vascular diseases are believed related to aerosol (Nel, 2005). Industrialisation and urbanisation have procreated anthropogenic emissions, substantially affecting health. A famous example is the 1952 London smog episode (December 1952- February 1953), and it has been estimated that about 12 000 excess deaths occurred during this period (Bell and Davis, 2001). The combination of smoke and fog led to the new, but now commonly used term *smog*, and has been attributed to the combination of high levels of SO_2 and particulate matter from domestic use of high-sulphur coal, in the presence of dense fog and very low, strong inversion.

2.4 Precursors to Secondary Organic Aerosol (SOA)

In most places, the sub-micron fraction of the atmospheric aerosol is dominated by organic compounds (Jimenez et al., 2009). A major fraction of the atmospheric organic aerosol is secondary organic aerosol (SOA), contributing up to 80 % of the total organics (Zhang et al., 2007). Depending on the location, time and specific source regions, SOA can be produced from both anthropogenic and biogenic volatile organic compounds (VOC). Despite some uncertainties, all estimations indicate a significantly larger production of biogenic secondary organic aerosol (BSOA) compared to anthropogenic secondary organic aerosol (ASOA) on a global scale (Spracklen et al., 2011; Kanakidou et al., 2005; Heald et al., 2010; Goldstein and Galbally, 2007), with estimated fluxes of 88 and 10 TgC yr^{-1}, respectively (Hallquist et al., 2009). Locally and regionally, however, the ASOA can supersede the BSOA (e.g. Fushimi et al., 2011; Steinbrecher et al., 2000; Aiken et al., 2009). The biogenic monoterpene emissions have been estimated to double the CCN number over boreal forests (Spracklen et al., 2008).

2.4.1 Emissions of Biogenic Volatile Organic Compounds (BVOC)

The characteristic scents of freshly picked herbs or of the Christmas tree, are examples of biogenic volatile organic compounds. The biogenic organic precursors to SOA studied in this thesis are emitted by vegetation with emphasis on boreal forest. The boreal forest is the world's largest terrestrial biome covering ~ 15 % of the Earth's land area in the northern regions. The dominating species belong to the genera *Abies* (fir), *Larix* (larch), *Picea* (spruce), and *Pinus* (pine). Deciduous species, e.g. of the genera *Alnus* (alder), *Betula* (birch), and *Populus* (poplar, aspen) are also represented in the boreal forest, particularly after disturbances like fires, windstorms or clear cuts where a large fraction of the forest is lost.

In the leaves or needles of the trees, the photosynthesis provides the energy to drive the chemical CO_2 fixation and other vital functions in the plant. The leaf surface is covered by highly specialized pores, *microscopic mouths* or *stomata*, where gas exchange of many substances occurs between the plant and atmosphere, e.g. water and gaseous compounds (CO_2, O_3, VOCs), see Figure 7. The stomata are formed by pairs of specialized guard cells, which perceive environmental signals and control the opening of the pore, playing an important role in allowing photosynthesis without letting the leaf dry out.

In addition to the primary carbon metabolites, plant cells include numerous compounds performing specialized functions. They are commonly known as secondary metabolites and can occasionally form a significant sink for fixed carbon. An important group of secondary metabolites is the isoprenoids, where isoprene is the back bone basic structural component of terpenes e.g. monoterpenes ($C_{10}H_{16}$) and sesquiterpenes ($C_{15}H_{24}$), see Figure 8.

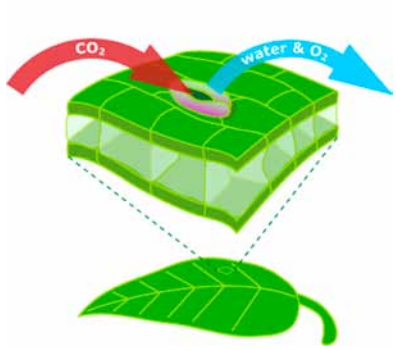

Figure 7: Carbon dioxide enters, while water and oxygen exit, through a leaf´s stomata. University of California Museum of Paleontology's Understanding Evolution (http://evolution.berkeley.edu).

Many isoprenoids are specifically synthesized for, e.g., defence purposes and stored in specialized storage tissues, although not all of their precise functions are yet understood. A protective role against high temperatures and reactive oxygen species such as ozone has been postulated for isoprenoids (Arneth et al., 2010).

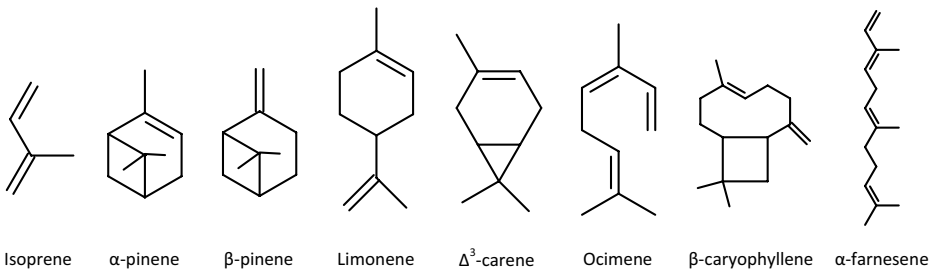

Figure 8: Chemical structures of typical biogenic VOC isporenoides.

Boreal trees have significant lower gas exchange during night when no photosynthesis can occur, and the stomata are closed. A significant part of the monoterpene emission originates from reservoirs, and their emissions may be controlled by temperature via the saturation vapour pressure of the compounds (Ghirardo et al., 2010). If the stomata are closed, the monoterpene emissions can be significantly reduced, in spite of large vapour pressure deficit. This is an example of physiological control over plant gas exchange.

The mixing ratio of BVOC in, or just above the forest depends on emission rates, (photo) chemical degradation and air mixing. Hakola et al., (2012) recently reported all year measurements of VOC at the SMEAR II station in Hyytiälä, Finland. The site is dominated by Scots pine forest, with some birch and spruce. The sesquiterpene concentrations were very low, only a few ppt. As some are very reactive, with atmospheric lifetimes of only a few minutes, not all of them can be measured in ambient air. Monoterpenes showed maximum mixing ratios in summer due to larger emissions during the growing season, in spite of their faster sink reaction.

During the winter months, the mixing ratios of biogenic compounds were very low (a few ppt), but increased gradually in spring, reaching a maximum in August (520 ppt and 2.3 ppt, mono- and sesquiterpenes respectively). Between April and October, the monoterpene mixing ratio showed diurnal variability, with highest (670 ppt) at night and lowest (60 ppt) during the day. Each monoterpene species also showed similar diurnal variation behaviour. The diurnal variation of monoterpenes was affected by the friction velocities, where the highest hourly concentrations were generally observed during the periods with the lowest friction velocities, and vice versa (Hakola et al., 2012).

The diurnal variation of isoprene concentration was opposite to the mono- and sesquiterpene diurnal curve. Isoprene is formed and emitted only in light conditions when the stomata are open, and therefore not emitted during the night. Due to its daytime maximum mixing ratios, isoprene dominated OH radical reactivity during summer (Hakola et al., 2012).

2.4.2 Emissions of Anthropogenic Volatile Organic Compounds (AVOC)

The characteristic scent of an old car on idle is an example of anthropogenic volatile organic compounds. In the late 1940's, an air pollution phenomenon began to impact the Los Angeles area. In sharp contrast to the *London smog*, this *photo chemical smog* or *Los Angeles smog* (Middleton et al., 1950) occurred on hot days with bright sunshine. Also crops were affected. The plant damage symptoms observed outdoors in ambient air could be replicated in the laboratory, by concurrently exposing plants to synthetic polluted air, containing alkenes (VOC) and nitrogen dioxide (NOx) in the presence of sunlight (*hv*), thus generating photo chemistry. This smog will be seen as a brownish haze that reduces the visibility in urban areas.

$$VOC + NO_x + hv \rightarrow \rightarrow O_3 + HNO_3 + PAN + HCHO + HCOOH + particles + \ldots$$

Anthropogenic volatile organic compound emissions include a wide range of compounds including hydrocarbons (alkanes, alkenes and aromatics), halocarbons (e.g. trichloroethylene) and oxygenates (alcohols, aldehydes, and ketones). Examples of anthropogenic volatile organic compounds (AVOC) are aromatic hydrocarbons e.g. benzene, toluene and p-xylene (Figure 9). VOCs are usually divided into non methane (NMVOC) and methane. A component of VOCs is ethylene, which is also a plant hormone that can seriously affect the growth and development of plants, in particular by promoting senescence (aging) (Wang et al., 2007).

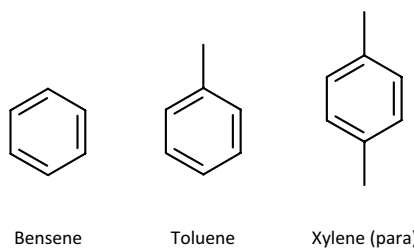

Figure 9: Chemical structures of typical anthropogenic VOC aromatic hydrocarbons.

The anthropogenic aromatic hydrocarbon concentrations can be comparable to the biogenic mono- and sesquiterpenes in concentration, even at a boreal forest dominated measurement site such as the SMEAR II station in Hyytiälä, Finland. Hakola et al., (2012) reported all year measurements of VOC, including aromatic hydrocarbons emitted by traffic and wood combustion (Hellén et al., 2008). The mean winter concentration of all aromatic hydrocarbons was 270 ppt, and after June below 100 ppt. The maximum concentrations in winter were attributed to slower sink reactions and larger emissions (e.g. heating with wood and cold starts of cars).

2.5 Atmospheric oxidation

2.5.1 Tropospheric ozone formation

The most important atmospheric oxidants in the troposphere are ozone, OH radicals (day-time), NO_3-radicals (night-time) and Cl (marine environment). In general, ozone and OH are the most important ones, while NO_3 can be significant during night time (Brown and Stutz, 2012). The combination of VOC, NOx and sunlight (*hv*) results in an increase of tropospheric ozone.

The main source of tropospheric ozone is the photolysis of NO_2. When NO_2 is photolysed to NO, atomic oxygen radical is formed, which will react with molecular oxygen to form ozone in the presence of a third body M (Finlayson-Pitts and Pitts, 2000).

$$NO_2 + hv\ (\lambda < 430\ nm) \rightarrow NO + O^{\cdot} \qquad \text{Reaction 1}$$

$$O^{\cdot} + O_2 + M \rightarrow O_3 + M \qquad \text{Reaction 2}$$

The ozone will quickly oxidise NO back to NO_2, and a steady state concentration of ozone will be obtained as a balance of reactions 1, 2 and 3.

$$O_3 + NO \rightarrow NO_2 + O_2 \qquad \text{Reaction 3}$$

However, in the presence of VOC, peroxy radicals (HO_2, RO_2) may be formed that competes with and replaces ozone in the oxidation of NO. This results in a net production of tropospheric ozone, and therefore are VOCs important in the tropospheric ozone formation.

$$\text{VOC oxidation} \rightarrow \rightarrow RO_2^{\cdot} + HO_2^{\cdot}\ \text{(peroxy radicals)} \qquad \text{Reaction 4}$$

$$RO_2^{\cdot} + NO \rightarrow NO_2 + RO^{\cdot} \qquad \text{Reaction 5}$$

$$HO_2^{\cdot} + NO \rightarrow NO_2 + OH^{\cdot} \qquad \text{Reaction 6}$$

The typical mixing ratios of ozone in the northern hemisphere are between 20-45 ppb (Vingarzan, 2004), while in e.g. highly polluted megacities such as Mexico City and Beijing, up to hundreds of ppb have been measured (Molina and Molina, 2004). During the last century, the rural ozone has doubled and is projected to increase further (Vingarzan, 2004). The lifetime of ozone is highly dependent on latitude, altitude and season of the year, as increased solar intensity and water vapour shorten the lifetime. Additional sinks of ozone are dry and wet deposition.

Ozone in the presence of water vapour and solar radiation will generate OH radicals that are highly reactive, with a lifetime of less than 1 s. The daytime concentration of OH is about 10^6 molecules cm^{-3} (Seinfeld and Pandis, 2006). Other sources of OH are the photolysis of H_2O_2 or HONO.

2.5.2 Oxidation of VOC

In addition to wet and dry deposition, VOCs are removed from the atmosphere by photolysis or chemical reactions. The chemical lifetime of VOCs depend on the reactivity of each compound and are diverse. In addition to the chemical structure and the presence of e.g. high NOx, physical factors like temperature, humidity and solar radiation can be important. Reactive, unsaturated VOCs have lifetimes of minutes, while some persistent compounds can stay for years. Several of the products formed in these reactions will take part in further reactions, and are often referred to as first and second generation products.

Radicals are important in atmospheric oxidation, which can be inorganic (e.g. OH, NO_3, Cl) or organic. In atmospheric degradation, three groups of organic radicals are often discussed; R alkyl-, RO alkoxy- and RO_2 alkylperoxy radicals. The predominant oxidation of VOCs during daytime is the reaction with OH radicals.

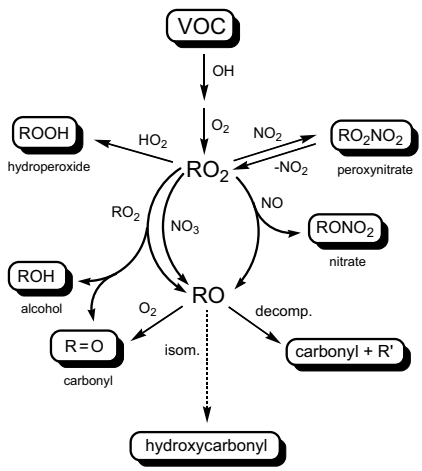

Figure 10: Simplified schematic of the OH initiated degradation of generic VOCs to produce first-generation products. Hallquist et al., 2009.

The reaction between the VOC and the OH radical starts by the abstraction of a hydrogen atom or addition to a double bond, forming an alkyl radical (R) and water. This is followed by a fast addition of O_2, generating a peroxy radical (RO_2), see Figure 10. At high NO conditions, the RO_2 is readily converted to an alkoxy radical (RO) via the oxidation of NO to NO_2. Larger RO_2 radicals can generate stable organic nitrates from the reaction with NO. At low NO_x conditions, the RO_2 reacts with HO_2 to form a hydroperoxide, or with another RO_2 to form RO, or products such as alcohol and carbonyls. The RO reacts, isomerises or decomposes to carbonyl or hydroxyl carbonyl products. The RO_2 radical can also be temporally trapped by the reaction with NO_2 to form peroxy nitrates e.g. peroxyacetyl nitrate (PAN), which can be transported long-range.

Another important atmospheric oxidant is ozone. Ozonolysis of alkenes has a fundamentally different mechanism, compared to radical initiated oxidation. The carbon to carbon double bond of an alkene is attacked and forms a primary ozonide (POZ), see Figure 11. This ozonide is unstable and decomposes into a carbonyl and a bi-radical, the Criegee intermediate (CI*) that is both vibrationally and electronically excited since the reaction is highly exotermic (Johnson and Marston, 2008). The excited CI* may have several fates, one is the Stabilized Criegee Intermediate (SCI) where the excited CI* is quenched to form a stabilized CI that can react with water or oxygenated organics. Another is the hydroxyperoxide channel where the excited CI* decomposes into reactive OH and an alkyl radical. The relative importance of the two reaction paths is dependent on the molecular structure of the parent alkene, and products from both have been identified in aerosol particles. Under atmospheric conditions, the SCI channel is often dominated by reaction with water vapour (Tobias and Ziemann, 2001).

The initial cleavage of the carbon to carbon bond of the primary ozonide in the ozonolysis reaction is a key feature. Oxidation can lead to both functionalization (addition of functional groups) and/or fragmentation. For acyclic and exocyclic alkenes with the double bound outside the ring structure, e.g. β-pinene, this cleavage leads to a smaller carbon skeleton that may offset decreasing volatility from the formation of functional groups.

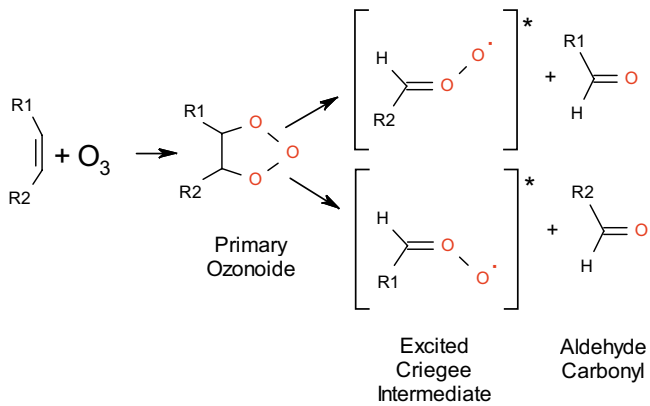

Figure 11. Initial mechanism of the ozonolysis of alkene.

This is contrary to endocyclic compounds where the double bound is located within the ring structure, e.g. α-pinene, where several functional groups can be formed by ozonolysis without fragmentation. Ozone reactions with aromatic hydrocarbons are of negligible importance.

2.6 Aerosol volatility

In chemistry and physics, *volatility* reflects the distribution between vapour and solid or liquid. The volatility of a SOA particle is the sum of the partial pressures of the compounds that are distributed between gas and condensed phase. The volatility of a compound is related to the saturation vapour pressure, the molar fraction and the activity coefficient in a non-ideal mixture. At a given temperature, a compound with higher saturation vapour pressure vaporises more readily than a compound with a lower saturation vapour pressure. The vapour pressure (concentration) of a compound can vary, but the saturation vapour pressure is a specific property of the compound.

The saturation ratio S, is the ratio between partial pressure and the saturation vapour pressure of the system at a given temperature. A gas is saturated when the partial pressure is equal to the saturation vapour pressure (S=1) and supersaturated when S>1.

Atmospheric reactions will generate oxidized products with polar functional groups that in general will have lower volatility compared to the reactants. In an aerosol, compounds will partition between the gas and the particle phase via evaporation and uptake according to its equilibrium. Changes in the composition of the gas phase will be reflected by changes in particle composition, and vice versa. Chemical aging processes in the condensed phase e.g. oligomerisation and formation of macromolecules, will therefore directly affect volatility (Vesterinen et al., 2007).

Since SOA consist of a significant fraction of semi-volatile compounds, the mass concentration is a function of the amount, volatility and the aerosol mass subjected for partitioning. The distribution of a semi volatile organic compound can be expressed using its partitioning coefficient K_p (Pankow, 1994), which is dependent on e.g. the temperature and the total aerosol particle concentration.

$$K_{p,\,i} = \frac{F_{i,\,om}}{A_i \times TSP} = \frac{R \times T \times f_{om}}{MW_{om} \times \zeta_i \times\ p_i^0} \qquad \text{Equation 1}$$

Where K_p is the partitioning coefficient for compound i. F_i and A_i are the particulate and gaseous concentrations of compound i, respectively. TSP is the concentration of total suspended particulate matter. R is the gas constant, T (K) is the temperature, f_{om} is the weight fraction of the TSP that makes up the absorbing om phase. MW_{om} is the mean molecular weight of all of the compounds in the om phase, ζ is the activity coefficient

in the om phase on the mole fraction scale, and $p_i°$ is the vapour pressure of compound i as a liquid at the temperature of interest.

As a consequence, dilution of SOA or increasing temperature will make the compound i to redistribute from particle phase into the gas phase, i.e. the chemical composition will change in both particle and gas until a new equilibrium will occur.

A way to express aerosol formation from organic aerosol precursor is the aerosol yield Y (Odum et al., 1996), as the fraction of formed organic mass (ΔM_{org}) to total amount of reacted hydrocarbon (ΔHC).

$$Y = \frac{\Delta M_{org}}{\Delta HC} = \sum_i Y_i = M_{org} \sum_i \frac{\alpha_i \times K_{om,\ i}}{1 + K_{om,i} \times M_{org}} \qquad \text{Equation 2}$$

Atmospheric oxidation of a parent precursor will form several products that in turn may be oxidised further. The stoichiometric factor (α) describes the amount of formed product i from the reacted precursor. The aerosol yield for product i (Y_i) with a low $K_{om,i}$ or when M_{org} is low, is proportional to organic aerosol mass (M_{org}) as the denominator will be 1. For non volatile product i (large $K_{om,i}$) or presence of large M_{org} the yield will be equal to α as the $M_{org} \times K_{om,i}$ in the numerator and the denominator will cancel each other. The non-stoichiometric nature of aerosol yields due to the partitioning is a known feature for SOA formation, and can be characterised by yield curves, plots of yield versus total organic aerosol mass.

2.6.1 Volatility representations

The aerosol yield from organic precursors can be described from all product yields (all α´s) and their volatilities (K_p's), that together form the volatility distribution of the products. It is, however, not feasible to sum up all semi-volatile compounds contributing to SOA. To handle this, the use of a two proxy products approach has traditionally been used to express the volatility from SOA forming reactions, see Figure 12 a-b. This two product model has been a useful tool to parameterise experimentally derived yield curves and to describe SOA in atmospheric chemistry models. In another approach, the Volatility Basis Set (VBS) presented by Donahue et al., 2006, a larger number of proxy products were used to represent a range of volatility. In this approach, the volatility distribution is represented by lumping all organics into respectively categories (bins) by their saturation vapour pressure, often expressed as (C^*_i , µg m^{-3}) and separated by factors of 10. C_i^* is the effective saturation concentration of the compound, and is the inverse of the Pankow type partitioning coefficient K_p. The size of each bin is corresponds to the sum of all contribution products yields (α´s). The bins represents proxy products of product yields (α´s), that can be transferred between gas and particle phase. A VBS often include nine bins, starting at C^* = 0.01 µg m^{-3} and ranging up to 10^6 g m^{-3}. Typical atmospheric condensed phase mass concentrations are between 1 and 100 µg m^{-3}.

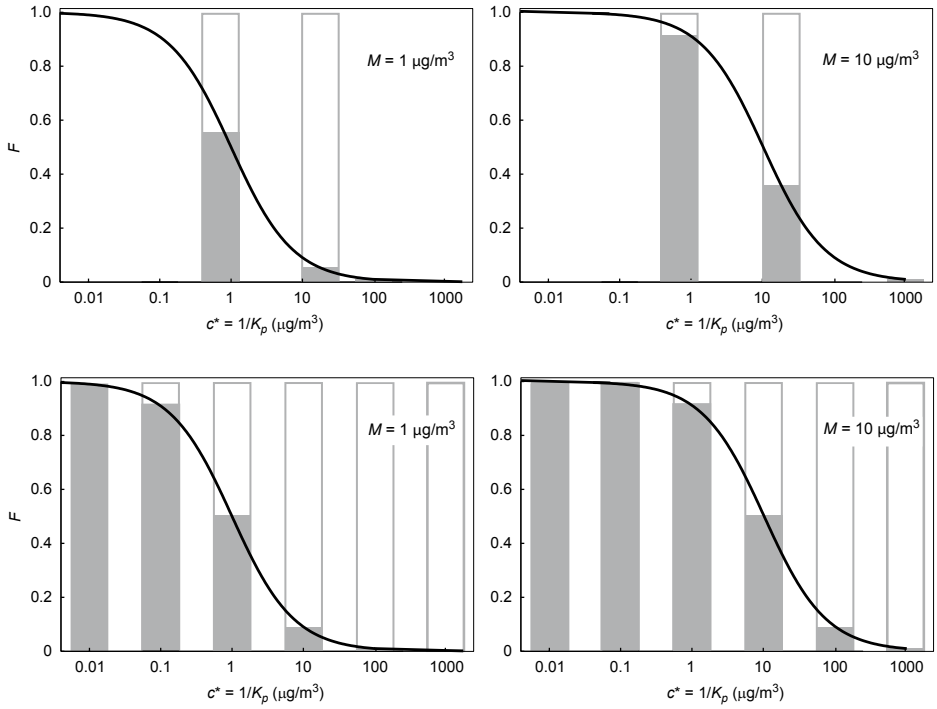

Figure 12: Representation of gas–particle partitioning for a complex mixture of semi-volatiles using (a–b) the 'two-product model', in which the semi-volatiles are represented by two model compounds with experimentally determined vapour pressures, and (c–d) the ''volatility basis set'', which employs a larger number of lumped compounds with prescribed vapour pressures. Partitioning at two mass loadings of organic aerosol (1 and 10 mg m^{-3}) is shown for each. Note that these plots only show the fraction F of each semi-volatile compound in the particle phase; particle-phase concentrations are obtained by multiplying F by total mass concentration of each semi-volatile (Kroll and Seinfeld, 2008).

The bins represents three volatility classes of VOCs; Low, Semi and Intermediate volatility. Low VOC (LVOCs): C*= (0.01, 0.1) µg m^{-3}. These compounds are mostly in the condensed phase. Semi-VOC (SVOCs): C*= (1, 10, 100) µg m^{-3}. These compounds will be found in both gas and condensed phases. Intermediate VOC (IVOCs): C*= (10^3, 10^4, 10^5, 10^6) µg m^{-3}. These compounds are almost entirely in the gas phase. There are two additional classes outside the VBS range, VOC: C* > 10^6 µg m^{-3} represents the vast majority of emissions and routinely measured organics. Non-VOC (NVOCs): C* <0.01 µg m^{-3}. These compounds are always in the particulate phase and can be placed in the first bin (0.01 µg m^{-3}) of the VBS (Donahue et al., 2006).

3 Experimental equipment and procedures

3.1 Aerosol characterization and data evaluation

3.1.1 Condensation Particle Counter (CPC)

The number concentration of aerosol particles can be monitored with a Condensation Particle Counter (CPC) (McMurry, 2000). In a CPC (Figure 13), the initial size of the sampled aerosol particles is increased by condensing a super-saturated vapour onto the surface of the particles, forming particles large enough to be detected with optical methods. The most frequently used liquids as the condensing vapour are alcohols (e.g. 1-butanol) or water. Several methods for producing super-saturation have been suggested, but the most widely used is the continuous flow conductive cooling type. Here the sampled particles are first exposed to a vapour at high temperature, and then brought into a cooled condenser where the super-saturated vapour condenses onto the particles. Subsequently, the droplets are counted optically.

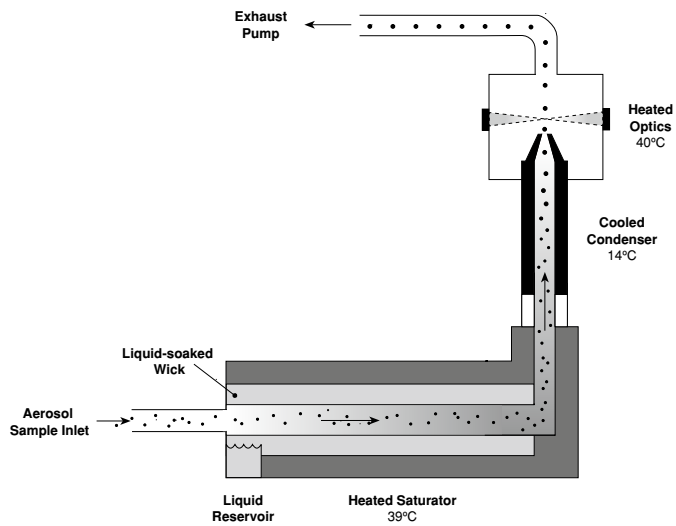

Figure 13: Schematic of a Condensation Particle Counter (CPC). Adapted from TSI Inc.

The lower size detection limit is mainly determined by the level of super-saturation generated inside the instrument, and can be fine-tuned by optimizing the temperature difference between the saturator and the condenser in the instrument.

3.1.2 Differential Mobility Analyser (DMA)

A selected size or the size distribution of aerosol particles can be extracted with a Differential Mobility Analyser (DMA) e.g., Liu and Pui, 1974; Winklmayr et al., 1991. A DMA classifies particles according to their aerodynamic mobility in an electrical field, see Figure 14. Since the DMA only can classify charged particles, the particles are brought to a known charge distribution, e.g. by a radioactive neutralizer (e.g., Ni-63, Kr-85) before entering the DMA. The charged polydisperse aerosol laminar flow enters a cylinder with a rod in the centre. By applying a voltage between the cylinder and the rod, an electrical field is created in which the charges particles move. Particles charged opposite to the rod will be drawn towards the centre, where the drag force to each particle is dependent on the shape and size of the particle. By setting a voltage of the centre rod, the particles with corresponding aerodynamic diameters can be selected and a monodisperse aerosol obtained. The size distribution of an aerosol can be measured using a Scanning Mobility Particle Sizer (SMPS), where the classifying voltage of the DMA is ramped in a continuous manner while the concentrations are monitored continuously using a CPC (Wang and Flagan, 1990).

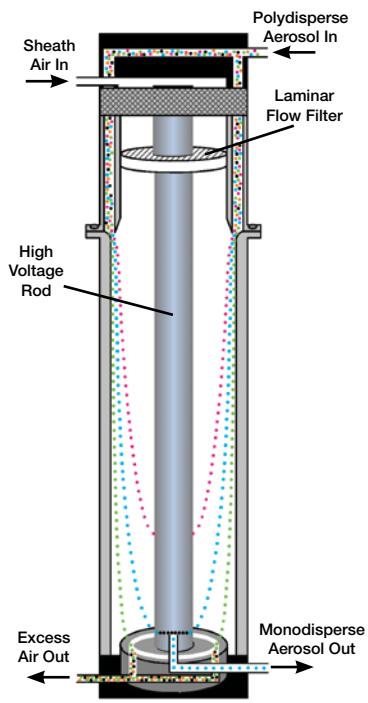

Figure 14: Schematic of a Differential Mobility Analyzer (DMA). Adapted from TSI Inc.

3.1.3 Volatility Tandem Differential Mobility Analyser (VTDMA)

A Volatility Tandem Differential Mobility Analyser (VTDMA) (Rader et al., 1987) is a useful set up to determine the thermal characteristics of aerosol particles, see Figure 15. The aerosol sample is dried using a Nafion® dryer, and a narrow range particle diameter (typically around 80 nm) is selected using a DMA operated in a re-circulating mode (Jonsson et al., 2007; Salo et al., 2011b). The size selected aerosol is then directed under laminar flow conditions through one of several temperature controlled paths in an oven unit. Each oven has a 50 cm aluminium block with an independent heating element. Typically temperatures applied are from 298 to 523 K ± 0.1 K in steps of 15 K. To enable swift changes in evaporative temperatures, the sample flow (0.3 SLPM) is switched between the ovens. The residence time is 2 sec in the oven, assuming laminar flow. During the relatively short residence time, the evaporation of the particles is under non equilibrium conditions (Riipinen et al., 2010). At the exit of the heated region, the evaporated gas is adsorbed by activated charcoal diffusion scrubbers to prevent re-condensation. Finally, the evaporated particle is classified using a Scanning Mobility Particle Sizer (SMPS). A wide range of temperatures, or one or a few running continuously, can be used for thermal characterisation of SOA. Using a VTDMA setup, nebulizing single compounds, it is also possible to determine vapour pressures and enthalpy of sublimation of e.g. carboxylic acids (Salo et al., 2010).

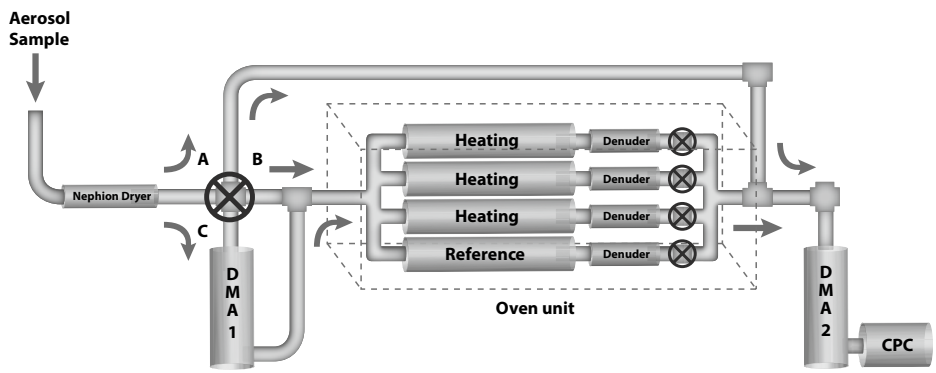

Figure 15: Schematic of a Volatility Tandem Differential Mobility Analyser (VTDMA). Three schemes can be applied. A: bypass of DMA1 and oven unit. B: bypass of DMA 1 in thermo denuder (TD) mode. C: size selecting VTDMA mode.

The median number diameter (geometric mean) of the heat exposed aerosol distribution, normalized to a defined reference diameter (D_{pRef}) derives the Normalised Modal Diameter (NMDp). Assuming spherical particles, Volume Fraction Remaining (VFR= $(NMDp)^3$) is obtained. NMDp and VFR are both related to a specific temperature, normally denoted as index, e.g. VFR(383K) as well as a defined reference size. An increase in NMDp(K) or VFR(K) corresponds to a less volatile aerosol particle.

To obtain more information from VTDMA data over a set of temperatures, VFR(K) or NMDp(K) can be presented as a function of temperature (K) on the x-axis, a so called thermogram. The temperature range of a SOA thermogram is typically 298 to 523 K in intervals of 15 K. The shape of the thermograms describes the volatility of all compounds in the aerosol particle. To obtain more information from the full range of evaporation temperatures, a sigmoidal Hill function curve (Hill, 1913) can be fitted a to the VFR(K) data.

$$VFR_T = VFR_{max} + \frac{(VFR_{min} - VFR_{max})}{1 + \left(\frac{T_{position}}{T}\right)^{S_{VFR}}} \qquad \text{Equation 3}$$

The slope factor S_{VFR} and the $T_{position}$ define the shape and the mid-position of the sigmoidal curve. VFR_{max} and VFR_{min} define the boundaries of the highest and lowest VFRs, respectively. The parameters add more information than from the individual VFR(K)s, and also make it possible to easily compare thermograms. In order to more strictly define the most volatile and the non-volatile fraction, Equation 1 can be used to derive e.g. VFR_{298K} and VFR_{523K}. In addition, the temperature where VFR is e.g. 0.5 ($T_{VFR0.5}$) can be calculated. The $T_{VFR0.5}$ is a general measure of the volatility, and an increase in $T_{VFR0.}5$ corresponds to a less volatile aerosol particle. The slope factor S_{VFR} is a measure of the distribution of particle components volatility, i.e. an aerosol with a steeper slope has a more narrow vapour pressure distribution of its major constituents, see Figure 16.

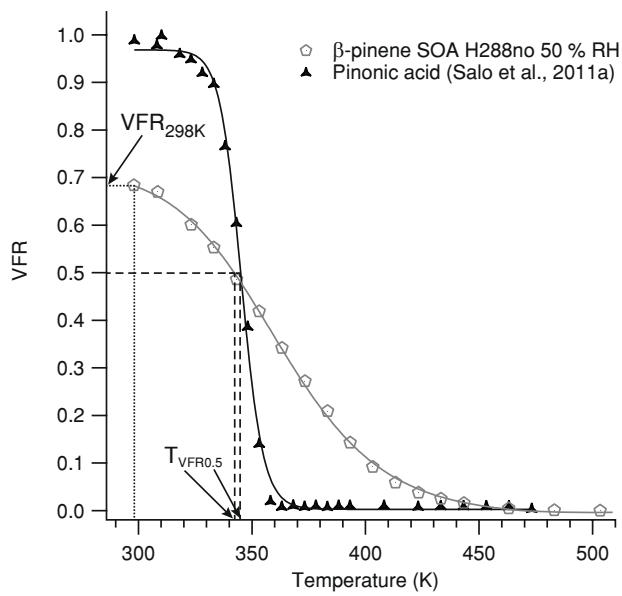

Figure 16: Plot of VFR against evaporation temperatures (thermogram) for pinonic acid and β-pinene SOA. Solid lines show the sigmoidal fits to the data, while dotted lines indicate VFR_{298K} and $T_{VFR0.5}$. The slope factor S_{VFR} is the steepness of the curves.

3.1.4 Aerosol Mass Spectrometer (AMS)

A Quadrupol Aerosol Mass Spectrometers (QAMS) can be used to determine the chemical composition of SOA (Aerodyne Research Inc., DeCarlo et al., 2006). QAMS measures mass spectra and chemically resolved size distributions of aerosol particles with unit mass resolution, and a time resolution of minutes.

After the inlet, the aerosol particles are focused via an aerodynamic lens, before entering into vacuum, where the aerosol size is determined in the particle time of flight region (P-ToF). The particles then hit a heated surface (~ 900 K), are evaporated and ionised using Electron Impact at 70eV before entering the orthogonal quadropole, where the chemical composition is determined from mass to charge ratio (m/z). The high temperature and energy in the ionisation step, results in significant fragmentation of the organic aerosol fraction, and single species can hardly be identified but provides a standardized fragmentation pattern that can be related to changes in chemical composition. Ion signals are integrated over all particle sizes, thus, the overall composition of the SOA is determined. SOA ageing are often referred to as m/z 44 (CO_2^+, strongly oxygenated fragment) to m/z 43 ($C_2H_3O^+$ and $C_3H_7^+$, less oxygenated fragments).

3.1.5 SOA density

The density of SOA is important for determine SOA yields from SOA mass. An estimation of the density of the SOA particles is difficult, as only 10-20 % can be attributed to certain organic compounds. By combining SOA mass and volume determine techniques such as AMS and SMPS, the effective density can be measured. The density provided by aerosol mobility-based techniques includes the effects of potential voids in the particles, and relies on the critical assumption that the particle density is independent of particle size. In the absence of direct measurements, it is recommended that a value of 1.4 g cm^{-3} is used for the SOA density (Hallquist et al., 2009), especially when determining SOA mass yields from measured volume concentrations. Elemental carbon has a density of approximately 2 g cm^{-3} (Seinfeld and Pandis, 2006).

3.2 Chambers - controlled reality

Between the field measurements and the modeling of atmospheric SOA, experiments in various reaction chambers enable a controlled reality. The chambers allow the study of atmospheric processes under controlled conditions e.g. temperature, pressure, light and composition of gases. The results and assessments of data from reaction chamber experiments contribute the larger part of our present understanding of SOA. These atmospheric mimicking experiments serve as an important link between fundamental studies on e.g. reaction kinetics of single compounds, to field observations and modeling of SOA. There are numerous chambers available around the world for the study of various atmospheric processes, each one with its special features.

A basic issue in all experimental studies concerns the design and properties of the experimental setup. The setups have different e.g. surface processes due to chamber wall material. For accurate evaluation of experimental data, each chamber needs to be well characterized.

Typically, the evolution of an aerosol can be studied over time, i.e. minutes, hours or days, in a static smog chamber. The SAPHIR chamber at Forschungszentrum Jülich, Germany is one such example. Selected gases are mixed in a sealed volume, and the developments of the reactions are followed with time. Another type of experimental setup applicable to detailed studies of SOA, is a laminar flow reactor, e. g. G-FROST at the University of Gothenburg, Sweden. The constant generation of SOA of a well-defined age can be characterized for a continued period of time, and gives the opportunity of detailed studies of a SOA fixed in age. A combination of a smog chamber and a flow reactor is the semi-flow/static plant chamber JPAC at Forschungszentrum Jülich, Germany.

3.2.1 G-FROST - measuring minutes forever

The G-FROST (Gothenburg - Flow Reactor for Oxidation Studies at low Temperatures) is located in the Department of Chemistry and Molecular Biology, University of Gothenburg. The setup (Figure 17) enables studies of oxidation of terpenes producing secondary organic aerosol (SOA) under controlled changes in e.g. temperature, relative humidity and reactant concentration. A constant aerosol production can be running for several days depending on the requirements, e.g. time needed for sampling or aerosol characterisation.

Laminar flow refers to when a fluid or gas flows in parallel layers, with no disruption between the layers. At low velocities, a fluid/gas tends to flow without lateral mixing, and adjacent layers slide past one another, like playing cards. There are no cross currents perpendicular to the direction of flow, nor eddies or swirls. In laminar flow, the motion of SOA is very orderly, moving in straight lines parallel to the tube walls. The Reynolds number (Re) can be used to estimate the motion of a gas or fluid. For a flow through a straight tube with a circular cross-section, the Re is generally defined by the diameter of the tube, the density and the mean velocity of the fluid or gas divided by the viscosity. When the viscous forces are dominant at $Re < 2\ 000$ the fluid or gas motion will ultimately be laminar, whereas at $Re > 4\ 000$ the flow is turbulent (Hinds, 1999).

The G-FROST facility is designed to deliver a stable and constant SOA, ranging from 0.01 to 100 μg m^{-3}. The vertical flow reactor is a 1.91 m long Pyrex® glass cylinder with a diameter of 10 cm, where the inner wall is coated with halocarbon wax to reduce the wall losses of reactive gaseous species. G-FROST is located in an insulated and temperature controlled outer chamber (2.0x2.0x1.5 m Kylma COMPACTA®) that gives the possibility to house measurement equipment at the desired temperature. The temperature can be varied between 243 and 325 K. Four temperature sensors are distributed vertically on the outside of the reactor, in addition to temperature measurements in the housing and in the sample flow. A vertical temperature gradient on the flow reactor can disturb the laminar flow.

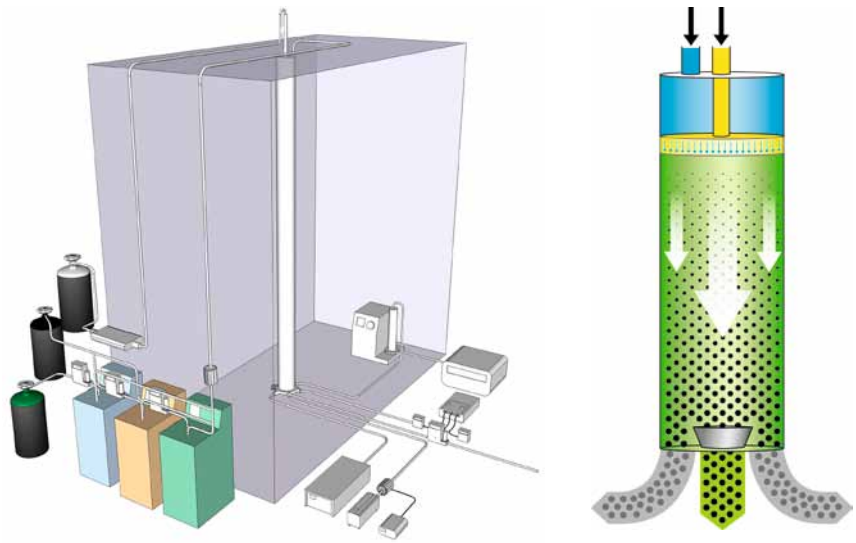

Figure 17: Schematic of Gothenburg - Flow Reactor for Oxidation Studies at low Temperatures (G-FROST). The whole setup (left), and a flow reactor (right).

The SOA precursor is delivered by a temperature controlled diffusion vial, typically in the concentration range 10–50 ppb with low variability. The unit is placed inside a wash bottle, placed in a temperature controlled bath (Julabo F25), with an mass flow controller (MFC) controlled flow of nitrogen (Nitrogen 4.8 AGA Linde Gas). The amount of organic compound is controlled by the temperature of the bath and the diameter of the diffusion vial glass tube. The main flow that carries the gaseous organic precursors enters through the top of the flow reactor. Before and after each experiment, the organic is sampled with absorption tubes (Tenax®) and analysed using GC-FID (Gas Chromatography-Flame Ionisation Detector Finnigan/Tremetrics 9001) with a two-step thermal desorption (Unity Thermal Desorber, Markes International Ltd.). The ozone is delivered through a sliding injector, where the end of the injector is equipped with a mixing unit for efficient mixing with the SOA precursor in the main flow. Ozone is generated using a MFC adjusted flow of oxygen (Instrument oxygen 5.0 AGA Linde GAS), passing through a UV-lamp unit (SOG-3, UVP). The typical applied ozone concentrations are in the range of 200 ppb to 10 ppm. Before and after each experiment, ozone is measured by a UV photometric ozone analyser (model 49C, Thermo Environmental Instruments Inc.). To investigate radical chemistry in the G-FROST facility, the addition of an OH scavenger (e.g. cyclohexane or 2-butanol) can be used. A MFC adjusted flow of nitrogen (Nitrogen 4.8 AGA Linde Gas) is passed through a temperature controlled wash bottle containing the OH scavenger.

The relative humidity (RH) can be set from < 0.1 % up to 85 %, with a variation of less than 0.1 RH-units at 298 K. The humidity in the system is controlled by temperature controlled diffusion, where MFC (Mass Stream M+W Instruments) flow of purified air (Laboratory Zero Air Generator Model N-GC6000 Linde Gas and Sofnox R, Molecular

Products Ltd.) is passed through a GORE TEX® tube (20 cm PTFE TA003, Gore), soaked in a bottle of purified water (Millipore Synergy 185), housed in a temperature controlled bath (Julabo F25). The humidity is controlled by the temperature of the bath, and the relative humidity is registered continuously prior entering the G-FROST by a relative humidity meter (Vaisala), as well as in the sample flow using a dew point meter (Optidew, Micell Instruments).

G-FROST has a pressure controlling device to minimize any disturbances due to fluctuation in ambient pressure. Since the total flow is regulated with mass flow controllers, any such fluctuation will change the reaction time and concentration of the reactants. The pressure within the flow reactor is regulated at the outflow by using a PID function (LabVIEW NI USB6229 National Instruments), adjusting measured pressure (PTB110 Vaisala) to a set value above ambient (PTA427 Vaisala), see Figure 18.

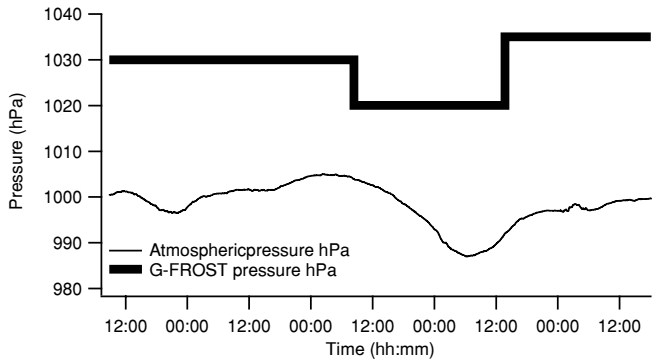

Figure 18: Atmospheric pressure and the pressure measured inside G-FROST using the pressure control system.

The rate constant k of a chemical reaction is often temperature dependent, i. e. when a new temperature is set in G-FROST, the ozone needs to be set according to the respective k if one wants to achieve the same rate of reaction. To compare initial conditions of ozonolysis of different organic aerosol precursors, the initial reaction rate can be obtained from the rate expression:

$$r = k \times [Terpene] \times [Ozone] \qquad \text{Equation 4}$$

Where k the rate constant, and r is the initial reaction rate when [Terpene] and [Ozone] are the initial concentrations of terpene and ozone, respectively.

At a new temperature (T) or pressure (P), the volume flow (V) needs to be adjusted according to the ideal gas law, to obtain the identical residence (reaction) time.

$$V_1 = V_2 \times \frac{P_2}{P_1} \times \frac{T_1}{T_2}$$ Equation 5

In a flow reactor, the SOA age can be fixed in time. Fluctuations in pressure or temperature will alter the volume flow and thus the reaction time in a flow reactor. The reaction time in G-FROST is typically 240 s, and can be varied (40-500 s) by the position of the mixing unit or by adjusting the flow. The bottom of the flow reactor has a sampling funnel, using only the centre part of the laminar flow. This reduces the impact of the slower flow near the walls of the flow reactor, which might be influenced by the surface. The reaction time in G-FROST can be calculated using the volume flows, the radius of the reactor and the length between the mixing unit and the sampling spot. Typical in- and sampling flows are 1.6 and 0.94 SLPM respectively (Jonsson et al., 2008b).

The centre of a laminar flow in a tube has maximum velocity, while the velocity is zero at the wall. The mean flow velocity ($\bar{u}$) is the volume flow (Q) divided by the cross section area (A) of the tube. (Douglas 1979). The maximum velocity (u_{max}) is two times the medium velocity ($\bar{u}$):

$$u_{max} = 2 \times \overline{u} = 2 \times \frac{Q}{A} = 2 \times \frac{Q}{\pi \times r^2}$$ Equation 6

Only the centre flow is used for analysis in G-FROST, i.e. the mean velocity of the sample flow has a higher velocity compared to the total flow. The velocity of the sampled flow can be calculated (Cengel, 1997).

$$u_{sample} = \frac{u_{max}}{r_{\max}^2} \times (r_{max}^2 \times r_{sample}^2)$$ Equation 7

In G-FROST, r_{max} corresponds to the radius of the flow tube and r_{sample} to the radius of the sample flow. By dividing the cross section area into small segments and calculating the mean velocity by each added segment, the accumulated volume flow that match the out flow gives the mean velocity of the sample flow $\bar{u}_{sample}$. The reaction time is the distance between the mixing unit and the sampling funnel divided by the mean velocity of the sample flow $\bar{u}_{sample}$.

In a typical experiment in G-FROST, both physical (temperature, pressure and residence time) and chemical (humidity, VOC, ozone and radical chemistry) parameters can be controlled. After stable conditions are reached, a selected parameter, e.g. humidity, can be altered and the potential response in SOA be characterised. The size distribution, particle number and mass concentrations are continuously measured using a SMPS system (3936L75, TSI). A VTDMA setup enables thermal characterisation.

3.2.2 SAPHIR

The large outdoor chamber SAPHIR (Simulation of Atmospheric PHotochemistry In a large Reaction chamber), enables studies of photochemical processes in the troposphere. The chamber, located at Forschungszentrum Jülich, Germany, is a cylindrical shaped double walled FEP-Teflon chamber (Rohrer et al., 2005 and in Bohn et al., 2005). The volume of the SAPHIR chamber is 270 m^3; the diameter is 5 m, the length 20 m and the area 324 m^2. The chamber has a louvre shading system that can be open fully or partly to enable daylight conditions, exposing the chamber to natural solar radiation (transmission 85 %), or closed to simulate dark conditions, inhibiting photochemical processes. The chamber is operated with synthetic air (Linde 6.0) and kept with an overpressure of about 50 Pa. A continuous flow of synthetic air maintains the over pressure and compensates for the sampling by the various analytical instruments. This flow, 7 - 9 m^3 h^{-1}, causes dilution of the reaction mixture. Synthetic air is also used to permanently flush the space between the inner and the outer Teflon wall. This, together with the over pressure of the chamber will prevent intrusion of contaminants.

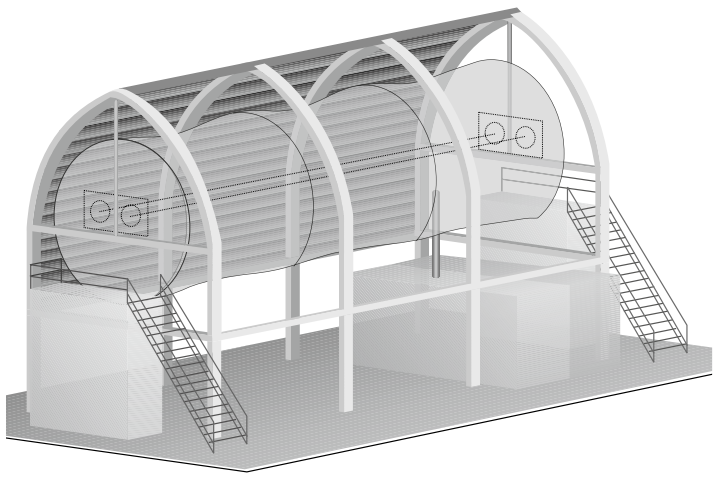

Figure 19: Schematic of the ambient light exposed static outdoor chamber SAPHIR, Forschungszentrum Jülich, Germany. Illustration by FZJ.

The SAPHIR chamber is equipped with various analytical techniques for gas measurements, ranging from radicals and intermediates to stable precursors, e.g. ozone (Chemiluminiscence), NO_x and hydrocarbons (GC-MS, PTR-MS) (Rohrer et al., 2005). The actinic flux and the associated photolysis frequencies are provided from measurements with a spectral radiometer. OH radicals were measured by Laser Induced Fluorescence (LIF), which allowed for establishing relations of aerosol properties and composition to the experimental OH dose. The OH dose is the integral of the OH concentration over time, and gives the cumulated OH concentrations to which gases, vapours and particles were exposed at a given time of the experiment. Particle number and number size distributions are measured by a CPC and a SMPS.

A typical experiment starts at early morning with addition of water in the closed chamber. After mixing, the SOA precursor/s is/are added and quantified using a PTR-MS. After additional mixing, e.g. ozone is added and the roof is opened without delay. With reactive SOA precursors, solar radiation generates particles (nucleation) that grow through condensation and coagulation until the mass maximum concentration is reached, normally within hours. At ageing experiments, the roof is typically closed in the evening and opened again in the morning. At the end of the experiment, the chamber is closed and flushed with synthetic air to prepare for next experiment.

3.2.3 Jülich Plant Atmosphere Chamber (JPAC)

In the Jülich Plant Atmosphere Chamber (JPAC), SOA from organic precursors from real plants can be studied. The chamber is located at Forschungszentrum Jülich, Germany, and an extensive description of the setup can be found in Mentel et al., (2009). A simplified schematic presentation of the system setup is shown in Figure 20.

The plants (about 1 m tall) are mounted with the stem through a sealed Teflon floor of a 1150 l Borosilicate glass chamber (plant chamber, PC). Lamps mimicking the solar spectrum provide a day/night light cycle, and purified air (particle, VOC, NOx and ozone free) with a controlled CO_2 concentration is continuously added to the PC. The VOC emissions are transferred to a second larger (1450 l) reaction chamber (RC), where the oxidation of the vapours and nucleation occurs. Two additional air flows are fed into the RC, controlling RH and ozone (typically 65 % and 90 ppb respectively). A UV lamp is placed inside the RC to produce OH radicals by photolysis of ozone in the presence of water.

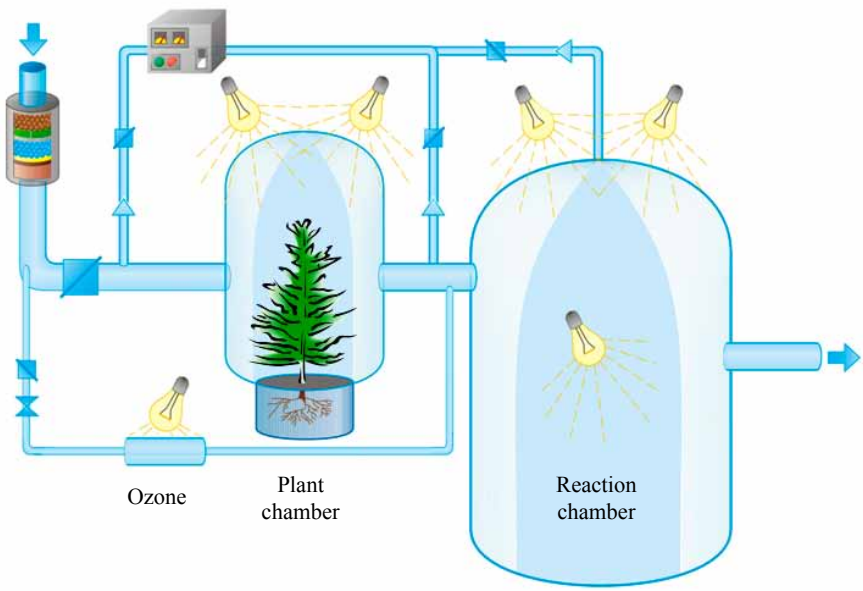

Figure 20: Schematic of Jülich Plant Atmosphere Chamber (JPAC), Forschungzentrum Jülich, Germany. Illustration by FZJ.

Both PC and RC have Teflon fans, providing a homogeneous mixture within minutes, and are mounted in separate climate-controlled housings (283 to 323 K). The residence times in the well mixed PC and RC are typically 20 and 65 min respectively.

In a typical experiment, the lamps are switched off at night time, and the plants emit low amounts of VOC. When the lamps are switched on in the morning, the VOC emissions increase, and after reaching a stable concentration in the RC (about noon), the UV lamps in the RC is turned on to generate OH. The VOCs are consumed and nucleation occurs. This first nucleation event, just shortly after the UV lamp is switched on, produces a narrow, fast growing particle mode. As the reaction mixture is diluted by continuous flush out, the available surface decreases and eventually is not enough for the continuously produced condensable vapours. Thus, after 2-3 h, a second, wider and quasi-continuous nucleation occurs. This second nucleation dominates the particle mass. Addition of non-plant emitted compounds can be added directly to the RC, possible affecting the chemistry of the SOA but not the plants.

4 Results

The ozonolysis mechanisms of the monoterpenes β-pinene (Paper I) and limonene (Paper II, Pathak et al., 2012) were studied with the aid of the G-FROST flow reactor. The investigated systems increased in chemical complexity, and combinations of biogenic VOCs (Paper IV) as well as mixed biogenic and anthropogenic VOCs (Paper III, Emanuelsson et al., 2012) were investigated in the large outdoor static smog chamber SAPHIR. Emissions from real boreal forest plants were studied in the Jülich Plant Chamber. The time scale ranged from minutes, when studying SOA formation in the G-FROST, to several days in the SAPHIR during ageing experiments.

Using a VTDMA-setup, the thermal characteristics of SOA were measured at a range of evaporation temperatures, where a sigmoidal fit to the data enabled parameterisation of the volatility properties (Paper I and IV). The parameters extracted were e.g. $T_{VFR0.5}$ and the slope factor S_{VFR}. These parameters are measures of the general volatility and the volatility distribution of the condensed phase products respectively.

4.1 Ozonolysis of β-pinene and limonene

The laminar flow reactor G-FROST was used for studies of the ozonolysis mechanism of the monoterpenes β-pinene (Paper I) and limonene (Paper II). The influence of humidity and radical conditions on SOA formation from three concentrations of β-pinene was investigated at 298 and 288 K. The experiments were designed to establish differences in ozonolysis mechanism between the exocyclic double bond compound β-pinene and previously investigated endocyclic monoterpenes.

At a lower experimental temperature, ozonolysis of β-pinene resulted in larger SOA mass and number, and the SOA got a broader volatility distribution. The effect of the varied parameters on number, mass and S_{VFR} is illustrated in Figure 21. From the data shown, it is evident that SOA mass and number always had a negative water effect, i.e. decreased with increasing water concentration (RH %). Generally, increased water concentrations gave a more volatile aerosol, as quantified by lower $T_{VFR0.5}$ and a more narrow volatility distribution, i.e. a steeper S_{VFR}. The radical conditions were controlled by the use of the OH scavengers cyclohexane and 2-butanol. Removing OH lowered both SOA mass and number, where 2-butanol had the strongest effect. This was valid for all conditions, i.e. water concentrations, temperatures and initial rates. When the slope S_{VFR} was steeper, lower mass and number of SOA were recorded.

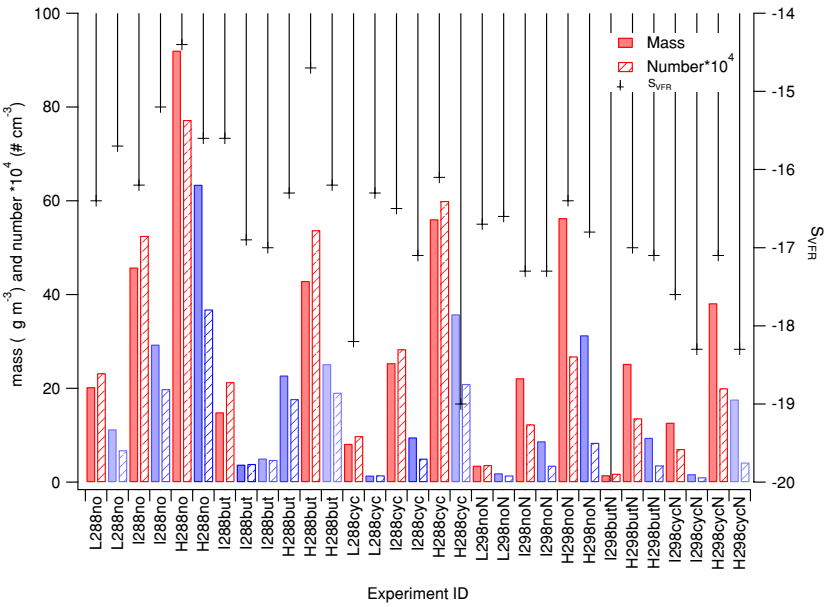

Figure 21: Ozonolysis of β-pinene in G-FROST (Paper I). SOA mass, number and slope factor SVFR at high ~ 50 % RH (blue) and low ~ 12 % RH (red), at three concentrations (L, I, H), 288 and 298 K, without OH scavenger, and with 2-butanol or cyclohexane. SOA mass and number decrease when decreasing SOA precursor concentration, increasing water concentration, increasing temperature, or using OH scavengers. The slope factor S_{VFR} is correlated to SOA mass and number.

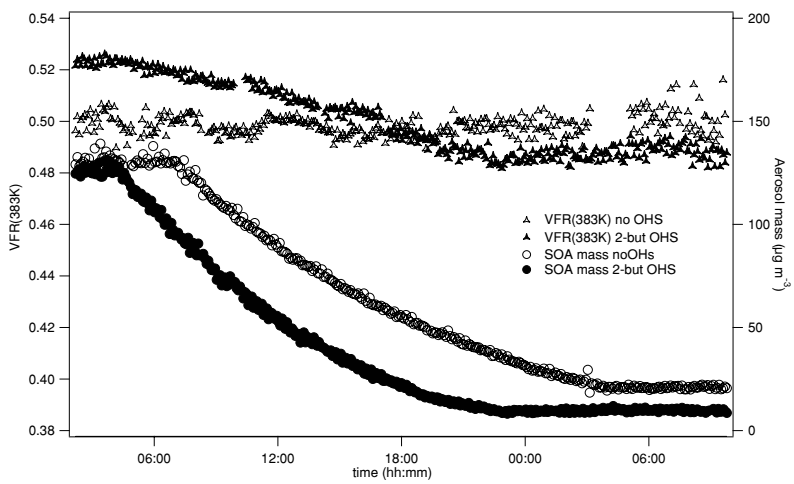

Figure 22: The effect on SOA mass and VFR(383K) by gradually decreasing the initial limonene concentration at a constant ozone concentration. Filled symbols indicate experiments with 2-butanol scavenger, while open symbols indicate experiments without scavenger.

With aid of G-FROST, VTDMA and FACSIMILE simulations, the ozonolysis of limonene, a monoterpene with two double bounds, one endo- and one exocyclic, was investigated (Paper II). SOA mass was strongly dependent on ozone concentrations and the presence of 2-butanol as OH scavenger. In the presence of a scavenger, the SOA volatility decreased with increasing levels of ozone, whereas without a scavenger, there was no significant change. At a fixed concentration of ozone while gradually decreasing the initial limonene concentration, as illustrated in Figure 22, the volatility reflected as VFR(383K) was unaffected in the absence of OH scavenger. With 2-butanol present, the volatility increased with decreasing limonene concentration. In ozonolysis of limonene, SOA mass increased and VFR(383K) decreased with increasing water concentration.

4.2 Ageing of SOA from mixed precursors

The outdoor smog chamber SAPHIR was used to study ageing processes and properties of SOA from relevant atmospheric VOC mixtures. In one set of experiments, SOA from compounds selected to mimic boreal forest emissions with typical mixtures of mono- and sesquiterpenes were characterised with respect to ageing over several days (Paper IV). Here, an AMS was integrated with the VTDMA system, enabling measurements of both chemical composition and volatility as a function of evaporation temperatures. Three sets of terpene combinations were used at 500-600 and 1000-1100 ppbC: One reference set of five boreal forest monoterpenes with equal amounts of α-pinene, β-pinene, limonene, Δ^3-carene and ocimene, a second set without ocimene, and a third with addition of the sesquiterpenes β-caryophyllene and α-farnesene. For reference, one ozone experiment in darkness without opening the roof, and one zero experiment without addition of any terpenes were conducted.

Figure 23 illustrates a typical SAPHIR BVOC experiment, where experimental time is displayed versus VFR, O/C, OH dose and SOA mass concentration. The particles start to form as soon as the roof opens and the gaseous mixture is exposed to sunlight. The AMS and SMPS instruments measured behind the ovens at a reference, or at elevated temperatures until the SOA maximum concentration had passed. The volatility, as measuring using a non-size selected thermo denuder $VFR_{TD/SAPHIR}$, decreased as the O/C increased. In the afternoon, both the first and the second day, typically 100 nm size selected VTDMA thermograms were measured, VFR_{VTDMA}. In the first evening, the roof was closed to be opened again in the morning. When the roof was open, the OH dose increased, as an effect of OH concentration.

The opening and closing of the roof is clearly visible in OH dose and O/C, both increasing when the roof is open. Aging, i.e. the production of less volatile (increasing VFR) SOA particles, with time was observed for all experiments. The exception is the second roof opening (indicated by the right hand vertical dotted line in Figure 23), where fresh oxidised material from gaseous phase is condensed on to pre-existing SOA particles, generating increased mass and a more volatile SOA.

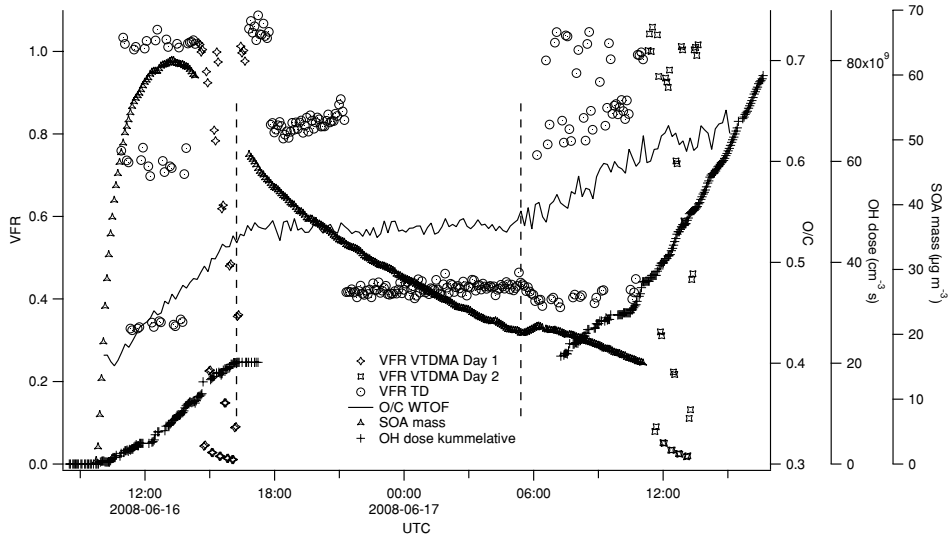

Figure 23: SOA ageing experiment in SAPHIR of boreal forest monoterpenes α-pinene, β-pinene, limonen, Δ^3-carene at initial concentrations of 1000 ppbC VOC and 43 ppb ozone. SOA mass concentration, OH dose, O/C and VFR are displayed. Size selected VFR from VTDMA in the temperature range of 298 to 573 K were measured once a day. Non size selected VFR(298K), (348K), and (398K) related to SAPHIR SMPS as $VFR_{TD/SAPHIR}$= ($Volume_{TD}$/$Volume_{SAPHIR}$) × ($Number_{SAPHIR}$/$Number_{TD}$) were measured continuously.

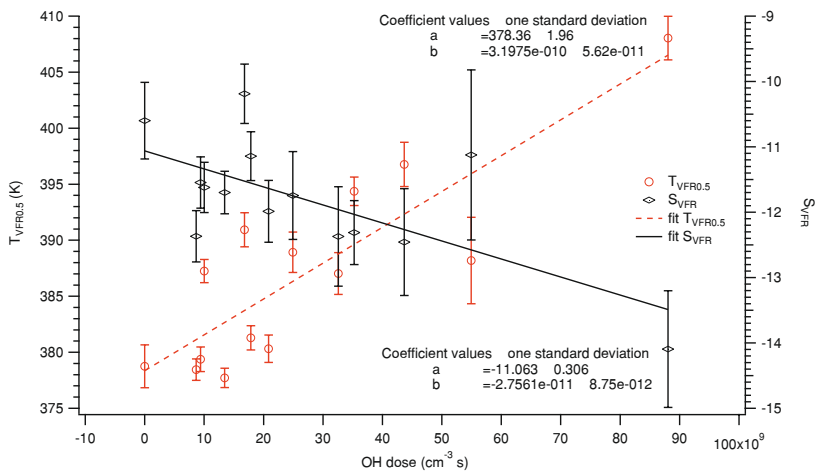

Figure 24: The relation between the OH dose and the parameters $T_{VFR0.5}$ and S_{VFR}, from sigmoidal fits of all thermograms from all combinations and concentrations of BVOCs in SAPHIR ageing experiments.

Sunny or cloudy conditions influenced the ageing effect, and BSOA became less volatile with increasing OH dose. Lumping of all experiments versus OH dose reveals the dependence of photo exposure. For all evaporative temperatures, there was an increase in VFR with OH dose (see fig 3a in Paper IV). Furthermore, the fitted $T_{VFR0.5}$ and S_{VFR} of the thermograms show a less volatile SOA and a less complex volatility distribution with increasing OH exposure in Figure 24. The volatility described by $T_{VFR0.5}$ increased by 0.3 % (ca 1 K) per hour of 1×10^6 molecule cm^{-3} of OH exposure. The slope factor S_{VFR} decreased by 0.9 % per hour of 1×10^6 molecule cm^{-3} of OH exposure.

Photochemical ageing of a BSOA was also characterised with combined volatility and mass spectrometric measurements (Paper IV). Photochemical ageing increased both Volume and Mass Fraction Remaining (in SMPS and AMS), and AMS fragment ratio m/z 44/43. SOA effective density also increased. High temperature exposure of SOA affected all m/z, where fraction of heavy fragments (m/z > 90) increased slightly.

The formation of anthropogenic SOA and its influence on biogenic SOA properties were studied in another set of experiments in SAPHIR (Paper III).To estimate the ASOA contribution, ASOA yields from experiments with individual aromatic SOA precursors were required. In the mixed Anthropogenic Biogenic Secondary Organic Aerosol (ABSOA) experiments, selected mixing schemes of AVOCs and BVOCs were applied. The reactivity, the sequence of addition, and the amount of the precursors influenced the SOA properties. Monoterpene oxidation products, including carboxylic acids and dimer esters, were identified in the aged aerosol at concentrations comparable to ambient air. When biogenic and anthropogenic precursors were added simultaneously (Figure 25), the VFRs at all measured temperatures increased during the experiments, both during light exposure and after closure of the roof.

The volatility reflected SOA processes. Figure 26 illustrates VFR(343K) of five combinations of AVOC and BVOC. To disentangle the effects of photochemistry, processes in the dark and anthropogenic contribution, VFR(343K) is displayed as function of experiment duration (upper panel) and OH dose (lower panel). In all panels, the size of the markers corresponds to the model-estimated anthropogenic fraction of SOA. VFR(343K) increases with increasing anthropogenic contribution, with pure BSOA at the bottom and pure ASOA grouping at the top of the VFR(343K) scale. The ABSOA experiment, wherein AVOC and BVOC were mixed from the beginning, is situated in between the pure systems in the graph. In the two cases when BVOC were added in the dark to pre-existing ASOA, a significant drop in VFR(343K) was observed. The formed ABSOA then becomes less volatile during the night, reflected as an increase of the VFR(343K). The lower panel displays the VFR(343K) as a function of the actual OH dose derived from OH LIF measurements.

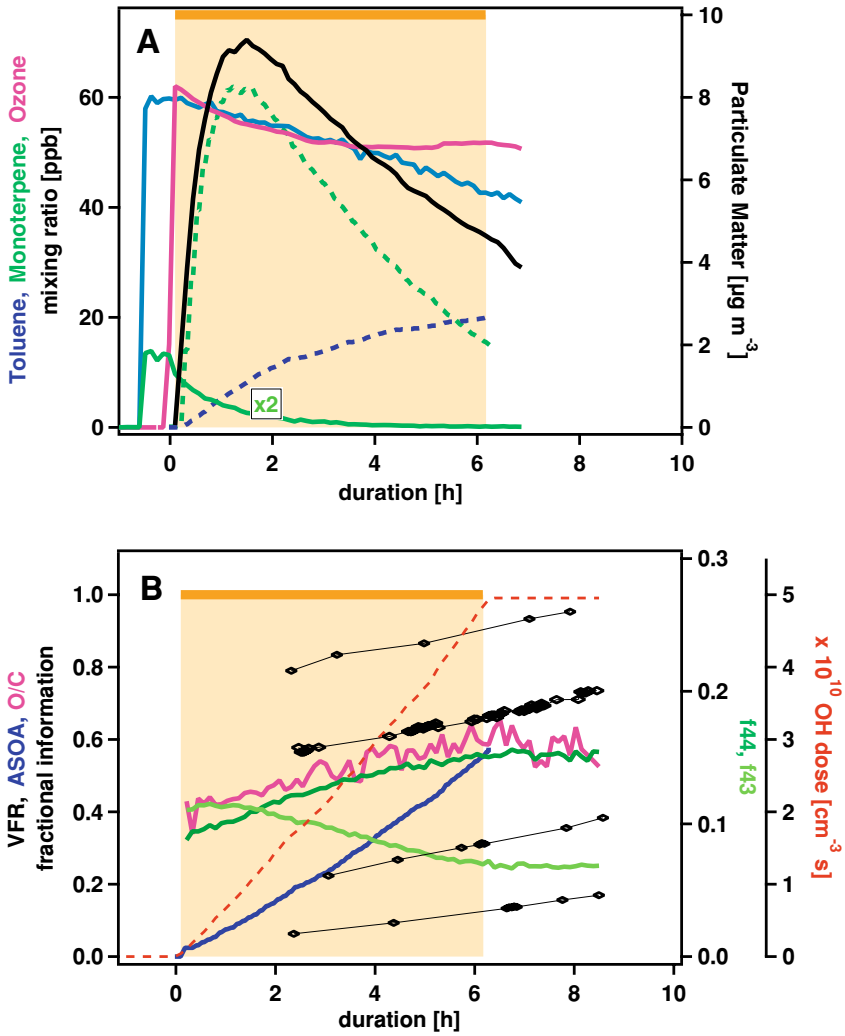

Figure 25: ABSOA experiment where biogenic (limonene and α-pinene) and anthropogenic (toluene) SOA precursors were added simultaneously 22/6 (Paper III). The top panel (A) shows the concentrations of reactants toluene (blue), monoterpenes (green), ozone (magenta), OH (red dashed) and produced SOA mass (black). The model derived biogenic (green) and anthropogenic (blue) SOA fractions are given as dashed lines. The bottom panel (B) shows the aerosol particle properties VFR(343K), VFR(373K), VFR(423K), VFR(463K) (black diamonds), O/C (magenta), f44 (dark green), and f43 (light green) together with model derived anthropogenic aerosol fraction (blue) and the OH dose (red dashed). The yellow area indicates light exposure with open roof.

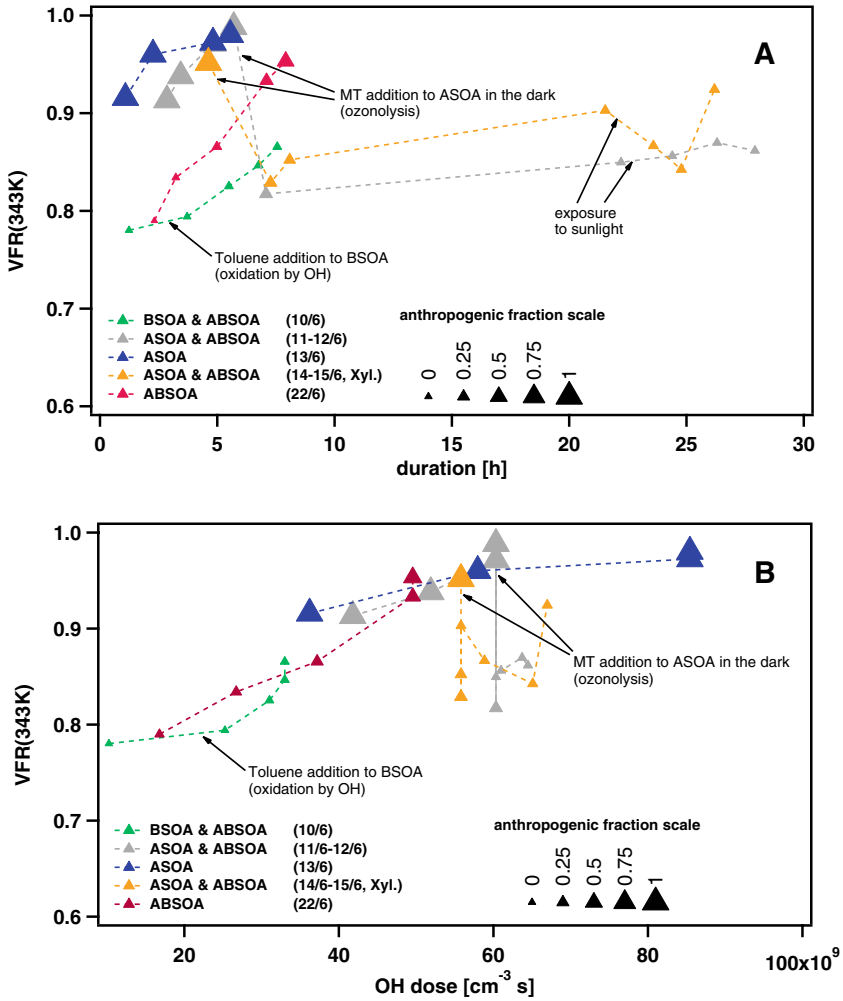

Figure 26: VFR(343K) for selected ABSOA experiments (Paper III) as a function of (A) elapsed time, and (B) OH dose. The size of the markers corresponds to the model-estimated anthropogenic fraction of SOA.

4.3 SOA from boreal forest emissions

The thermal properties of BSOA from real plant emissions were characterised using the Jülich Plant Chamber (not yet published). One campaign studied SOA from a boreal forest exposed to elevated temperatures. The air temperature of a light exposed mini boreal forest, two pines (*Pinus sylvestris*), one spruce (*Picea abies*) and one birch (*Betula pendula*), in the plant chamber was varied (288, 293 and 298 K). In on one set of experiments, the plants were kept in the dark at 305 K.

When the plants were exposed to light and kept at 288 and 293 K, no significant difference in $T_{position}$ and S_{VFR} could be measured. When the temperature was enhanced to 298 K, however, the SOA became more volatile ($T_{position}$ deceased) and got a wider distribution (increased S_{VFR}). When the plants were exposed to 305 K but no light, the volatility was comparable to 298 K and light, but S_{VFR} decreased i.e the SOA became more uniform.

A second campaign studied the influence of selected anthropogenic VOCs added to VOCs emitted from a mini boreal forest. At this campaign one pine (*Pinus sylvestris*), one spruce (*Picea abies*) and one birch (*Betula pendula*) were kept at light and 288 K in the plant chamber, and xylene was added to the emitted BVOCs in the reaction chamber.

In this campaign, the thermal properties of both 80 and 140 nm SOA particles of the two nucleation modes were measured. There was no significant difference between the two nucleation modes, but the 140 nm particles were less volatile and had a more uniform composition compared to the 80 nm particles within each mode. The pure xylene SOA had higher volatility and an obviously less complex composition. An increased amount of xylene added to the BVOCs slightly increased the volatility.

5 Discussion

The results are discussed mainly in terms of SOA particle mass, number and thermal properties as $T_{VFR0.5}$ and S_{VFR}. A high $T_{VFR0.5}$ temperature indicates low volatility, i.e. products with low saturation vapour pressures. Vapour pressure is dependent of molecular polarity and size, and in general a lower volatility implies a higher degree of oxidation. A steeper S_{VFR} is a measure of a more uniform volatility with lower complexity. A future research challenge would be to quantitatively estimate the chemical composition of the SOA particle from these parameters.

Most likely, SOA from VOCs is not only dependent on the type of organic precursor and oxidant, but also on the chemical and physical conditions. Some of the relevant parameters in studies of SOA are the concentration of water vapour and radicals, as well as temperature. The properties and processes involved in the formation and ageing of atmospherically relevant SOA are of large interest when it comes to climate modelling. The chemical mechanistic routes of SOA constituents might seem to be digging into details when it comes to global modelling, but are vital in the chemical understanding of the processes building the large-scale pattern.

In a future climate a temperature increase of 3.5 K year 2100 compared to 2000 (Scenario A2 IPCC, 2007) has been suggested. This will change the atmospheric aerosol load but the only possible way to estimate this is through modeling using present knowledge. Here the information on SOA thermal properties will be of high relevance. Furthermore, it can be expected that both gas and aqueous phase organic reactions will gain in importance in future climate, as elevated temperature increase biogenic emissions and possibly RH (Ervens et al., 2011)

5.1 Formation and thermal properties of secondary organic aerosol

5.1.1 Water vapour

A negative water dependence on SOA mass and number was observed for all investigated conditions for ozonolysis of β-pinene in G-FROST (Paper I). The water effect was related to a change in thermal properties where humid conditions provided a more volatile aerosol. The water effect on volatility for the β-pinene was further illustrated by the two distinctive groups of data relating the volatility distribution (S_{VFR}) to volatility ($T_{VFR0.5}$), see Figure 4 Paper I. In general, experiments at low water vapour pressure (humidity) had lower volatility (higher $T_{VFR0.5}$) and a more complex volatility distribution (less steep S_{VFR}) compared to experiments at high water vapour pressure.

Water as an active participant in SOA formation has been studied for various terpene systems, but the observed effect is not consistent, and seems strongly dependent on the chemical structure of the parent compound (Jonsson et al., 2006; 2008a). The water effect on SOA formation has been attributed to shifts in chemical reaction paths. Other possibilities are the physical water uptake of the SOA, and the change in partitioning of organic compounds between gas and condensed phase (Cocker et al., 2001). In ozonolysis, the excited Criegee intermediate can be collisionally stabilized to generate a stabilized Criegee intermediate (SCI) (Johnson and Marston, 2008). The SCI can react with e.g. water, carbonyl compounds and SO_2. Under atmospheric conditions, the bimolecular reaction of the SCI with water is expected to dominate due to the high concentration of water relative to organic carbonyls (Winterhalter et al., 1999).

Recent reinvestigations of the atmospheric importance of the SO_2 – SCI reaction, first suggested by Cox and Penkett 1971, proposed that for large SCI this latter reaction can compete with the water reaction (Mauldin et al., 2012). The water vapour concentration (i. e. not RH directly) influences the SOA formation via water dependent reaction paths. If a water reaction is fast, the increase in humidity will make this path dominant on the expense of others, and thus reduce the optional reaction paths. At low humidities, the water and non-water dependent reactions paths will have similar reaction rates, resulting in products with a larger distribution in vapour pressures. Water as an active component in ozonolysis opposes the use of RH % as an experimental measure of water concentration. The relationship between water vapour concentration and RH is strongly dependent on temperature. A certain level of RH can represent a wide range of water vapour concentrations/partial pressures dependent on temperature.

As described above, the atmospheric fate of SCI from ozonolysis can be determined from the concentrations and the corresponding rate coefficients of the potential reactants. The SCI fate is typically assumed to be determined by the reaction with water and, for some substitutions, the thermal reaction generating OH (Johnson and Marston, 2008; Tillmann et al., 2010). The reaction rate for water and SCI depends strongly on the substitution pattern of the SCI. This was indicated in the experimental results from ozonolysis of monoterpenes in G-FROST (Paper I and II). Experimental and theoretical studies have shown that SCI can react with organic compounds, mainly carbonyl compounds, alcohols and acids. Furthermore, the rates of these reactions with SCI depend on the structure and stereochemistry of the SCI. Unimolecular reactions of SCI depend strongly on the chemical structure, and forming hydroperoxide is likely to increase in importance with an increasing complexity of the SCI (Vereecken et al., 2012). The stabilization of the COO group of the SCI from β-pinene is most likely higher compared to the α-pinene, as the primary carbon is higher substituted. This effect is demonstrated by the negative water response of β-pinene in Paper I.

5.1.2 Radicals

The radical conditions can be altered in the laboratory by use of OH scavengers (e. g. 2-butanol or cyclohexane), providing systems without OH radicals with different $[HO_2]/[RO_2]$ ratios. Cyclohexane generates lower $[HO_2]/[RO_2]$ ratios than 2-butanol.

The produced SOA mass and number from ozonolysis of β-pinene was always in the following order: without scavenger >> cyclohexane > 2-butanol. This was valid for all conditions (humidities, temperatures and concentrations). An increase in $[HO_2]/[RO_2]$ resulted in a lower production of SOA and a decrease in aerosol volatility, as demonstrated by higher $T_{VFR0.5}$ and lower VFR_{298K} (Paper I).

The scavenger effect on volatility for the β-pinene was further illustrated by three distinctive groups of data; see Figure 4, Paper I. The non-OH scavenger cases (OH and ozone exposure) have the most diverse volatility distribution (the least steep slope, S_{VFR}). The experiments with cyclohexane as OH scavenger (ozone and low $[HO_2]/[RO_2]$) group at the least diverse volatility distribution, while 2-butanol (ozone and high $[HO_2]/[RO_2]$) is between the two groups. The presence of OH radicals makes chemistry more complex, and thus a production of compounds with a wider distribution in vapour pressures is expected.

The SOA volatility from limonene in the absence of an OH scavenger (2-butanol) was not affected by the ozone concentration, while in the presence of an OH scavenger, SOA volatility decreased with increasing ozone concentrations (Paper II). Multiphase ozonolysis involving secondary ozonide formation has been suggested for limonene (Maksymiuk et al., 2009). This can explain the results with a scavenger, which showed that VFR(383K) and the SOA mass increased with increasing ozone concentrations. The observed increase in VFR(383K) with limonene concentrations provides further indications of a second oxidation step, involving reaction of ozone with the primary products. For both high ozone and high limonene concentrations, the primary unsaturated products and SOA would be formed rapidly, enabling multiphase ozonolysis during the contact time in the flow reactor. However, the change in VFR(383K) with precursor concentrations was not observed in the absence of a scavenger. If the OH radical, by being a much more reactive oxidant, can inhibit ozone multiphase reactions, this will lead to OH addition instead of a formation of the secondary ozonide. Thus, the effect of ozone on volatility will be reduced, which was clearly observed in the non-scavenger experiments.

The FACSIMILE simulations of limonene ozonolysis (Paper II) showed that the product distribution was affected by changes in both OH and ozone concentrations. This partly explained the observed changes in volatility, but was strongly dependent on the estimation methods of the vapour pressures of the SOA constituents. The comparison between model an experiment indicated a need to consider organic peroxides as important SOA constituents. The formation of peroxyhemiacetals from monoterpenes has been demonstrated both theoretically (Jenkin, 2004) and experimentally (Docherty et al., 2005). For the exocyclic monoterpenes, an elevated $[HO_2]/[RO_2]$ ratio increases the potential for forming highly volatile hydrogen peroxides at the expense of less volatile ditto. A higher volatility makes the hydroperoxides more distributed towards the gas phase, and reduces the potential for reaction with carbonyl compounds to form peroxyhemiacetals. This implies that organic peroxides are important in SOA formation, mainly through the formation of the hemiacetals. This would explain the scavenger effect on SOA formation for β-pinene, as observed in Paper I, in addition to modelled experiments in Paper II.

On the SOA particle surface, a competition for reaction sites between OH and ozone is plausible. In flow reactor experiments reported by Renbaum and Smith 2011, the radical concentrations influenced the rates of the gas-particle reactions, but not the gas-phase-only reactions. Ozone is believed to saturate the surface of the liquid particles and to inhibit the OH reactions (Renbaum and Smith, 2011). The radical- and oxidant chemistry are not to be considered as independent, as the HO_2, RO_2, OH and ozone reactions affect SOA formation differently (Paper I). The experimental findings in Paper II could be explained by secondary condensed phase ozone chemistry, which competes with OH radicals for the oxidation of primary unsaturated products. If ozone diffuses into the condensed phase, the POZ can be generated, but the two fragments will react to generate SOZ due to mass transfer limitations. The diffusion of ozone in a liquid is limited compared to the gas phase, but is drastically reduced if the SOA particle is in a glassy state (Koop et al., 2011). Then, oxidation is likely to be considered primarily as a surface process.

SOA formation in the flow reactor may be mass transport limited during the relatively short reaction time of minutes, which potentially would underestimate the production of SOA under conditions with less mass transport limitation. The explicit modelling of evaporation and adsorption for limonene ozonolysis products (Paper II) indicated that the first generation products reached equilibrium between gas and condensed phase during the time in the flow reactor. In some cases, there was a deviation from equilibrium at the end of the flow reactor for the secondary products produced from ozonolysis of the first generation products. These calculations are based on partitioning into liquid droplets, and as pointed out by Virtanen et al., 2010, this assumption might not be valid for larger particles. BSOA generated in G-FROST is most likely not in glassy state, as the reaction time is on the scale of minutes and the SOA is easily evaporated. As there is only one double bond in β-pinene, mass transport limitations are less likely.

5.1.3 Temperature

A lower reaction temperature in the ozonolysis experiments with β-pinene enhanced the nucleation, generating SOA particle number size distributions with a higher peak, slightly shifted towards smaller diameters compared to the higher temperature (see Figure 2, paper I). The total SOA mass was also higher at 288 than 298 K.

A variation of the temperature will change the absolute water concentration, saturated vapour pressures, kinetics and plausible mass transfer within the particle. Partitioning theory suggests that lower temperatures would increase SOA as a physical effect, as semi-volatile components favour the condensed phase. When lowering the temperature at a fixed pressure, identical water vapour concentrations would result in an increase of relative humidity.

The homogeneous nucleation rate has a strong non-linear dependence on saturation ratio S. Therefore, nucleation is often perceived as an on-off process. The saturation ratio S is controlled by two factors, the actual concentration and the volatility of the compound, i.e. of the saturation concentration. The heat of evaporation (ΔH_{vap})

determines the sensitivity of the saturation concentration to temperature. The greater the heat of evaporation, the more sensitive is S to changes in temperature. An increase in the number of carbon atoms in a molecule and polarity also increases the heat of vaporisation. Typical aerosol constituents have ΔH_{vap} in the range of 90-150 kJ mol^{-1} (Salo et al., 2010). Volatility, and thus S, for large hydrocarbons is strongly temperature dependent. Shifts in experimental temperature will also influence the reaction rate via its activation energy (Ea), the energy barrier that must be overcome in order for a chemical reaction to occur. Addition and radical reactions often have small and sometimes negative Ea, being typical examples of barrier less reactions. The temperature effect on vapour pressure is thus expected to supersede the potential effect from the reaction rate for atmospherically relevant VOCs.

The effect of increased SOA when lowering the experimental temperature has been reported in several other studies of terpenes (e.g. Saathoff et al., 2009; Pathak et al., 2007). Pathak et al., attributed the temperature effect of β-pinene to the partitioning of products rather than to changes in chemistry. This is in line with our observation that experiments with higher mass had a less pronounced temperature effect. Thus, the relationship between SOA yield and organic aerosol mass is proportional to organic mass at low concentrations, and independent of organic mass at high concentrations.

5.1.4 Ozonolysis mechanisms for endo- and exocyclic terpenes

The flow reactor with precise control of e.g. temperature, pressure, humidity, initial reaction and radical conditions is an excellent setup for detailed mechanistic studies. In previous studies in G-FROST, it was suggested that endocyclic monoterpenes (e.g. α-pinene) behaved differently compared to exocyclic (e.g. β-pinene), both regarding the effect from water vapour concentration and radical chemistry (Jonsson et al., 2006, 2008b).

The position of the double bond is expected to influence the chemistry and the associated observed effects on SOA formation. In addition to the initial formation of two fragments from exocyclic β-pinene, the position of the substituents will impact plausible reactions. In order to explain the experimental finding in response to water vapour and radical conditions, there is a need to update the currently available ozonolysis mechanism. In the ozonolysis of β-pinene, the most reasonable explanation to our experimental findings, is the recently suggested decomposition of the stabilized CI via the hydroperoxide channel, see highlighted arrow in Figure 27 (Ngyen et al., 2009; Zhang and Zang 2005; Drozd and Donaue, 2011). Our results support this path of SCI from ozonolysis of β-pinene, as this reaction path will explain the water dependence, and partly also link to the radical effect (Paper I).

Limonene has both an endo- and an exocyclic double bond, where the initiated ozone addition will predominately be to the higher substituted endocyclic double bond. The remaining exocyclic double bond in limonene might be oxidised further down in the reaction cascade, and can also be related to condensed phase reactions. This would be a difference between the reaction of the exocyclic double bonds in limonene and β-pinene.

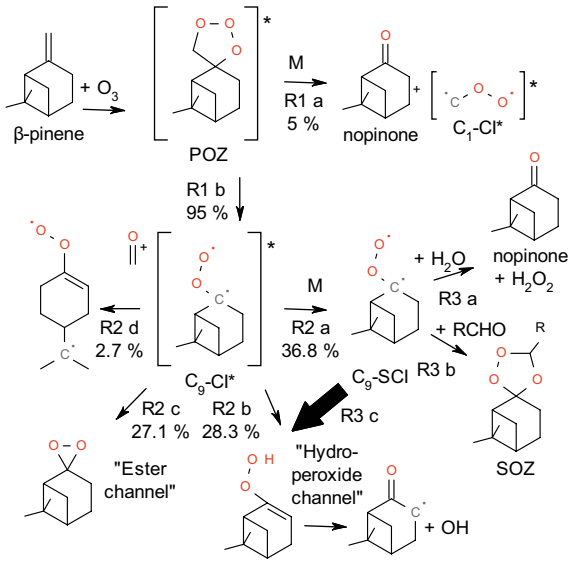

Figure 27: Major reaction paths in the ozonolysis of β-pinene. The routes and yields are from Nguyen et al., (2009) omitting isomers and paths with yields below 1 %. The reactions of the SCI (R3 a and R3 b) were suggested e.g. by Winterhalter et al., (1999). Our findings support an alternative path of the SCI, R3 c highlighted arrow.

5.1.5 SOA precursor concentration

The initial reaction rate is dependent not only on the rate coefficient, but also on organic SOA precursor and oxidant concentrations. For the three initial rates from different concentrations of β-pinene (in Paper I), the ozone concentrations were matched when lowering the reaction temperature to keep the three initial reaction rates fixed. For β-pinene SOA in Paper I, S_{VFR} has a weak concentration dependence where low concentrations tend to have a steeper slope compared to high concentrations. This would be in agreement with partitioning theory, which claims that the aerosol will have more different compounds contributing to the SOA particle at low temperatures and higher concentrations. Also, ASOA yields in the SAPHIR chamber increased with the organic aerosol load (Paper III) as expected from Raoul's law (Pankow, 1994).

When the ozone concentration was increased, the number size distributions of limonene were gradually shifted to lower diameters (insets Figure 1b and c in Paper II). SOA particle number concentration is dependent on how fast new particles are formed, i.e. how fast and how much chemistry generates products with sufficiently low vapour pressures. The rate of nucleation is strongly dependent on the saturation pressure. SOA is dependent on the product vapour pressures and the absolute concentrations of precursors (reactants and products) that can be dispensed between condensed and gaseous phase.

5.1.6 SOA formation potential of VOC

The potential of a VOC to generate SOA is dependent on the chemical structure, as SOA formation is dependent on the rate of degradation and the volatility of the produced products. Bernard et al., 2012 used a flow reactor setup to measure the upper limit nucleation threshold of ozonolysis of four monoterpenes. The concentrations were ranging from 3.9×10^{10} to 6.2×10^{9} molecules cm^{-3} (1.56 to 0.26 ppb), and could be ordered with respect to their SOA formation potential; α-pinene < myrcene < limonene < sabinene. β-pinene was not included in this study, but is expected to have a higher nucleation threshold, and lower SOA formation potential from chemical structure and rate constants.

The rate constant for the four VOCs limonene, α-pinene, β-pinene and toluene versus OH and ozone are listed in Table 1, together with their corresponding lifetimes, assuming representative atmospheric concentrations of OH and ozone. The two double bond molecule limonene has the shortest lifetime. The effect of the position of the double bond within the chemical structure is visible comparing α- and β-pinene that have the double bond in endo- and exocyclic position respectively. The lifetime regarding OH for α-pinene is slightly longer compared to β-pinene, while versus ozone the lifetime of β-pinene is more than a day compared to hours for α-pinene. Toluene has the longest lifetimes of the two oxidants. If only ozone was available, the toluene in the exhaust

Table 1: Rate constants k and lifetimes for OH and ozone for selected SOA precursors.

SOA precursor	VOC rate constant k (cm^3 $molecule^{-1}$ s^{-1})[a]		Lifetimes	
	OH	O_3	OH[b]	O_3[c]
limonene	17.1×10^{-11}	2.0×10^{-16}	49 min	2.0 h
α-pinene	5.37×10^{-11}	8.66×10^{-17}	2.6 h	4.6 h
β-pinene	7.89×10^{-11}	1.5×10^{-17}	1.8 h	1.1 day
toluene	5.96×10^{-12}	4.1×10^{-22}	23.3 h	110 years

[a]Atkinson 1994
[b]Assumed OH radical concentration: 2.0×10^{6} molecule cm^{-3},12-h daytime average. Atkinson and Arey 2003
[c]Assumed O3 concentration: 7×10^{11} molecule cm^{-3}, 24-h average. Atkinson and Arey 2003

from the first Ford T-model would fade away in 2018.
As shown in Table 1, the anthropogenic example toluene has a long atmospheric lifetime compared to the terpenes. It will thus have the potential to gradually increase the anthropogenic SOA portion, both long-term and far away from the source. A wide range of kinetics and lifetimes of the SOA precursor adds challenges when evaluating mixed SOA. The combinations of BVOCs representatives (in Paper IV) had a limited impact of SOA properties. As with variation within a narrow group, the experimental differences in e.g. OH dose will probably dominate the impact on SOA. When AVOC and BVOCs were mixed (in Paper III), the differences in chemical SOA potential

between the VOC precursors added complexity. In terms of evaluating the potential synergy effect of ABSOA, the slower but increasing contribution from AVOCs had to be considered. The anthropogenic fraction had to be evaluated from separate experiments to estimate the impact on ABSOA.

Hildebrandt et al., 2011 found that ABSOA derived from mixtures of AVOC and BVOC can be treated as ideal mixtures, and the yields can be parameterised applying the assumption of a common organic phase for partitioning. Consequently they suggest that ASOA and BSOA in the atmosphere interact by partitioning and that the presence of anthropogenic SOA enhances the concentrations of biogenic SOA, which then has important implications for environmental policies.

In the detailed studies of β-pineneozonolysis in the flow reactor, the slope factor S_{VFR} was more related to mass and number of produced β-pinene SOA, compared to VFR_{298K} and $T_{VFR0.5}$ (Paper I). When the slope is steeper, lower mass and number of SOA was recorded (see Figure 21). It is not clear if the slope gets less steep due to the large amount of SOA produced, or if a wider volatility distribution provides larger mass and number.

5.2 Ageing and thermal properties of secondary organic aerosol

5.2.1 Oxidative ageing

Ageing of organics associated with SOA involves a large number of pathways, intermediates and products. This chemical complexity makes precise measurement and prediction of the oxidation dynamics of the formation and ageing of atmospheric organic aerosol difficult. A general feature of the oxidation of organics is the formation of products with lower vapour pressures, i.e. lower volatility. Oxidative ageing of VOCs have been studied in several studies (e. g. Tritscher et al., 2011 and Donahue et al., 2012).

Ageing of mixed biogenic VOCs in the SAPHIR (Paper IV) was reflected as increasing VFR and oxygen to carbon ratio O/C with photo exposure (see Figure 23). In experiments with AVOC and BVOC (Paper III), the anthropogenic aerosol had higher O/C and was less volatile than the biogenic fraction (Figure 26). However, in order to produce significant amounts of anthropogenic SOA, the reaction mixtures needed a higher OH dose that also increased O/C and provided a less volatile aerosol. When heating BSOA particles, AMS analysis gave some indication on bias towards higher masses in the residual aerosol (paper IV). However, the effect was not as large as one could expect and is in line with the study of Cappa and Wilson (Cappa and Wilson, 2011), where essentially no spectral difference was observed as a function of temperature for α-pinene SOA.

Ageing is closely related to the oxidation state of SOA, but may not be captured by O/C as the oxidative state does not necessarily need to involve oxygen. One example is the oxidation of an alcohol to a carbonyl that is not reflected in O/C, but in the entity average carbon oxidation state ($\overline{OS}$) (Kroll et al., 2011) (Paper II).

5.2.2 Non oxidative ageing

In ageing experiments in the SAPHIR of mixed ABVOCs, the volatility decreased (VFR(343K) increased, Figure 26) overnight in the presence of low ozone concentrations (Paper III). Since O/C, f44, and f43 were levelling off when the roof was closed (duration > 6 h), the processes lowering volatility are likely non-oxidative with respect to oxygen content. The VFR(343K) continued to increase after the roof was closed, consistently for all investigated ASOA and ABSOA systems (Figure 25). One toluene experiment was exposed to more OH than the others, but still showed indications of ageing under dark conditions, however weaker. This ageing under dark conditions is likely due to chemical or morphological changes not affecting O/C. This phenomenon indicates a slow non-photochemical, non-oxidative ageing process, and could be an oligomerization by condensation reactions. Since the volatility of ABSOA decreases in the dark, the daytime enhancement may also have non-oxidative contributions. Night time ageing processes were previously reported by Tritscher et al., (2011) for α-pinene SOA, and are in line with our observations.

By definition, SOA is the combination of gaseous and condensed phases. But to refer to the condensed phase of SOA as simply not a gaseous phase is a coarse simplification. The type of condensed phases has large effects on e.g. the reaction kinetics, mass transfer and surface tension. In gas-to-particle partitioning models developed for SOA, the condensed phase is generally assumed to be in liquid state (Pankow, 1994; Odum et al., 1996). However, very limited information is available on the morphology and phase state of SOA particles. The physical state of the particles has a large impact on the condensed phase chemical reactions. One way to characterise the physical state is by investigating the particle bounce properties, where both elastic properties and surface properties affect their bounce probability. Studies of biogenic SOA have indicated that particles in the size range 17-30 nm bounced less than particles > 30 nm, which were characterised as amorphous solids (Virtanen et al., 2010). Thus, the initial nucleation process and growth of the newly formed particle is driven by mass transfer of molecules from gas phase to liquid phase. When the particles are more aged, the phase transfer to the amorphous solid phases takes place and the partition process changes (Virtanen et al., 2011).

The phase state of SOA particles from biogenic and anthropogenic precursors has been found to be affected by the relative humidity, where most types of atmospherically relevant SOA formed amorphous solid or semi-solid particles at RH <~ 60 %. The humidity induced phase changes were more related to the average molar mass of the SOA, compared to O/C or the CCN activity κ (Saukko et al., 2012). As the saturation vapour pressure is strongly related to molecular size, this non-liquid behaviour will most likely be reflected in a generally lower volatility.

5.2.3 Gas-phase ageing

Even after 24 h ageing in the SAPHIR chamber, gas phase ageing of SOA-precursors is clearly visible. The effect of opening the roof, both during the first and the second day of the ageing experiments of VOCs (see Figure 23), was reflected in increased SOA mass. The effect of fresh low volatility products condensing onto pre-existing SOA in SAPHIR ageing experiments were observed as a temporary lowering of VFR for both BSOA and ABSOA, i.e. a temporary increase in volatility (Paper IV and III). VFR recovers and exceeds the value before light exposure, indicating that the ageing process continues after the production of fresh material has ceased, forming an even less volatile SOA. This is consistent with previous results emphasising the importance of gas phase chemistry in the OH radical induced ageing of SOA (Salo et al., 2011a).

SOA in the SAPHIR is diluted during night. According to partitioning theory, dilution will transfer semi-volatiles from a condensed to a gaseous phase. When the roof is opened, these compounds will be oxidised by OH, and subsequently condense onto the remaining SOA particles. In the morning, the increasing temperature will decrease this effect, as higher temperatures from partitioning will distribute the semi-volatiles back towards the gaseous phase. The corresponding dip in VFR when opening the roof the second morning was not seen in cases where the extra photo-oxidation did only add a small increase in SOA mass.

In Paper III, the addition of BVOC onto pre-existing ASOA in the dark resulted in a significant drop in VFR (Figure 26). The drop in VFR was due to condensation of fresh BSOA material arising from the ozonolysis of the BVOC, as ozone was available from the previous photochemical processes. The fresh BSOA component generated a more volatile ABSOA aerosol, which became less volatile after addition during the night.

5.2.4 VOC mixtures

Detailed studies of a well-defined system (e.g. β-pinene and ozone) enable a mechanistic understanding of key processes. In order to consider more atmospheric realistic conditions, there is a need for studies of more complex system. Using such systems, one may achieve information that can be used to derive model parameterisations to match atmospheric observations. In mixed systems, containing several compounds participating in SOA formation, realism in parameterisation of SOA is gained on the expense of mechanistic resolution.

To improve understanding of the effects of complexity in SOA precursors, a set of experiments with a mixture of biogenic and anthropogenic SOA precursors with varying sequence of addition were conducted in the SAPHIR chamber (Paper III). An increase of the anthropogenic fraction and the OH dose provided an aerosol with higher O/C ratio and lower volatility. In ABSOA, already small fractions of ASOA increased VFR(343K), even at low degrees of oxidation. This indicated that ASOA components had a lower volatility, but also that they may trigger an extra ageing, either by oligomerisation or morphological changes e.g. the formation of glassy states (Zobrist et al., 2008; Virtanen et al., 2010).

Over the latest decade, the SOA community has taken interest in the impact from anthropogenic contributions on SOA. Using a combination of global modelling and observations of organic aerosol (AMS) and organic carbon (filters), Spracklen et al., (2011) proposed a new source attribution of SOA. According to their analysis, the majority of the SOA may have biogenic precursors, but is strongly related to the anthropogenic tracer CO. Thus, this portion of SOA is called anthropogenic enhanced SOA. Such effects were proposed earlier by de Gouw et al. (2005, 2008) and de Gouw and Jimenez (2009). Our experimental findings show that ABSOA get a lower volatility, and contributes to the understanding of anthropogenic enhancement. The lower volatility induced by ASOA (and OH dose) has an influence on the atmospheric SOA lifetime. The BSOA fraction in mixed ABSOA is thus expected to have longer lifetimes and abundance in areas influenced by anthropogenic aromatic emissions, compared to BSOA regions. The products from aromatic systems and OH are expected to deviate (e.g. producing glyoxal) compared to monoterpenes, producing e.g. C_{10}, C_9 acids and peroxides.

Ageing experiments of selected combinations of the boreal forest monoterpenes and sesquiterpenes were performed with aid of the SAPHIR chamber (Paper IV). The effect on volatility from mixtures of BVOCs was only minor. This is probably due to too similar mechanisms and properties of the different terpenes. The effect of the OH dose seems to supersede the effect of the composition of terpene mixtures.

In the experiments of SOA from a mini boreal forest in the Jülich Plant Chamber, BSOA from plants exposed to 298 K were more volatile and less uniform compared to those exposed to 288 and 293 K. Higher temperature would imply larger emissions of BVOC if only physical processes would constrain emissions. But the plant can actively control gas exchange through the stomata, e.g. to oppose dehydration. As SOA from 288 and 293 K had similar thermal properties, the BVOC emissions at those temperatures are probably similar, but different from those at 298 K. This can imply a more active regulation of stomata at 298 K. The stomata are mostly closed when photo synthesis cannot occur. Plants kept at higher temperature but in dark, generated less complex BSOA. Thus the BVOCs emitted though the stomata are most likely to be BSOA precursors, and have vapour pressures different from the compounds not emitted through the stomata.

On the first day, the ageing experiments of boreal mono terpenes in SAPHIR have comparable volatility, and are slightly less complex, compared to the plant chamber experiments. But on the second day, the aged SOA in SAPHIR has become distinctly less volatile and more uniform. The residence time in the JPAC reaction chamber is about an hour; thus the SOA is expected to resemble a fresh SAPHIR SOA and vice versa. The lover volatility and the more uniform composition of the larger SOA particles can be an indication of a non-liquid physical state. This is in agreement with the indications of BSOA formation of glassy, reflected as bouncing behavior discussed in section 5.2.2 (Saukko et al., 2012; Virtanen et al., 2011).

5.2.5 OH dose

In ageing experiments in the SAPHIR chamber, the OH dose showed to be a major driving force of SOA ageing, reflected as a decrease of volatility and a more uniform composition with an increasing OH dose.

VFRs from all investigated BVOC combinations in the SAPHIR experiments plotted versus the corresponding OH dose (Figure 3a Paper IV) show that increased VFR (less volatile SOA) is related to OH dose. This overall trend implies that, in general, the volatility of BSOA in models can be lumped together, and atmospheric ageing of SOA can be related to OH dose. The sigmoidal fit of the thermograms between 298 and 573 K from the BSOA systems, showed increasing $T_{VFR0.5}$ and a steeper slope S_{VFR} with an increasing OH dose (Figure 24). Thus, the SOA becomes less volatile and more uniform in its chemical composition. This was anticipated to the oxidation of the volatile fraction of the aerosol since it is more susceptible to gas phase OH reaction, while the low volatile fraction do not react with gas phase OH and the surface/bulk oxidation processes are to slow in comparison.

Also in the ABSOA experiments, the OH dose showed to be a good representative of ageing properties. (Paper III). Figure 26 displays the VFR(343K) as a function of time (A) and the actual OH dose (B) derived from the OH LIF measurements. The lowest dose on the scale corresponds to 1.5 h exposure to average atmospheric OH levels of 2×10^6 cm^{-3}, whereas the largest dose corresponds to 12 h exposure. To produce a significant anthropogenic aerosol fraction, the systems needed exposure to large OH doses, corresponding to oxidation over several hours at mid-European photochemical conditions. The larger OH dose also influenced the chemical composition, as evidenced by higher concentrations of dimer esters and second generation products in the particles. The results imply that the ageing and formation of less volatile ABSOA particles, reflected as an increase of VFR, is generally related to the OH dose, thus to photo-chemistry. The influence of the photo-chemistry on the BSOA components is also reflected in increasing second generation products, and to a lesser extent, the dimer fraction.

6 Conclusions

This thesis describes the work done to increase the knowledge of processes and properties of atmospheric relevant secondary organic aerosol (SOA) of both biogenic and anthropogenic origin. The common methodology of these projects is the VTDMA setup, which in combination with other observations has generated insight into both detailed chemical mechanisms, and physical processes that eventually could be suitable for testing air quality or climate models. During the course of this work the experimental facility G-FROST and the VTDMA setups, as well as corresponding data evaluation methodology, have been improved and refined.

The thermal properties could be linked to both formation and ageing processes of SOA. Using a VTDMA setup, where the thermal characteristics of SOA was measured at a range of evaporation temperatures, a sigmoidal fit to the data enabled parameterisation of the volatility properties. The parameters extracted were e.g. $T_{VFR0.5}$ and the slope factor S_{VFR}, which are measures of the general volatility and the volatility distribution of the condensed phase products, respectively. An increase in $T_{VFR0.5}$ indicates a decrease in volatility, while an increase of S_{VFR} states a broader distribution of vapour pressures. The response on these parameters from changes in experimental conditions could be linked to processes occurring both in the gaseous and the condensed phase. In photo-chemical experiments the change in $T_{VFR0.5}$ and S_{VFR} could be described using the OH dose.

The gas phase processes were found to be very important for SOA ageing, demonstrated to be driven mainly by OH exposure. However, processes in the condensed phase such as plausible non oxidative ageing processes and non-liquid behavior of SOA particles were also observed.

Detailed studies of ozonolysis of the boreal monoterpenes β-pinene and limonene were enabled by the precise control of reaction conditions using a flow reactor. The experimental findings in response to e.g. water and radical conditions emphasized the difference in ozonolysis reaction paths between endo- and exocyclic compounds. The results support the recently suggested decomposition of the stabilized Criegee Intermediate via the hydroperoxide channel in ozonolysis of β-pinene.

This thesis started with the naive question: *Physics and chemistry, aren´t they the same thing?* Physics and chemistry are not the same thing. Their paths differ, but they meet, among other fields, in the volatility of SOA. Collaboration and combined insights between chemistry, physics and biology are important factors in extending the knowledge of atmospheric science.

7 Acknowledgements

Acknowledgements blir på svenska erkännande eller bekräftelse. När jag nu skriver denna sista sida i min avhandling är det är många som förtjänar båda. På den långa men varken särskilt raka eller utstakade vägen är det åtskilliga som gjort mig följe. Jag vill börja med alla lärare och handledare som under över mina tjugo (!) år inom utbildningsväsendet väckt min nyfikenhet och förundran, som utmanat, stöttat och utvecklat. De senaste bland dessa är min handledare Mattias, biträdande handledare Håkan och min examinator Evert som kompletterat varandra och gjort det möjligt att skriva dessa rader.

Ein großes Dankeschön an alle meine Freunde und Kollegen, die in den Messkampagnen in Deutschland teilgenommen haben und einen grosser Beitrag zu dieser Abhandlung geleistet haben. Die Messkampangen waren nicht nur lange Arbeitsstunden und Apfelschorle, sondern auch große und kleine Abenteuer wie Konzerte, wackelige Radtouren, und Partys sowohl mit Kölsch, Spargel und als auch Nobelpreisträger.

En stor del av resan har även alla både nuvarande och tidigare kollegor och kurskompisar. Alla timmar med stora och små problem som vi löst med både enkla och kanske även ibland onödigt komplicerade lösningar. Det är i labbet jag trivs som bäst och med hjälp av bromsrör och silvertejp lämnar jag nu över det laminära flödet i goda händer som jag vet kommer vårda det väl.

Min familj och vänner som jag tyvärr ofta prioriterat bort den här sista tiden betyder så mycket för mig. Jag vet och känner att ni alltid finns bakom mig vad jag än tar mig för och jag ser verkligen fram emot att umgås mer med er.

Marcus var den som visade mig tidningsannonsen om att atmosfärsvetenskap sökte en doktorand och som uppmuntrade mig att ta steget. Det var nog ingen av oss som förstod vad det skulle innebära men du har alltid funnits där och när jag behövt det som bäst gett mej extra energi genom att gå på en bra konsert, leta upp en cash eller klia en get. Det bästa loppisfyndet har vi framför oss.

This work was founded by the Tellus research platform at University of Gothenburg. Kungl. och Hvitfeldska stiftelsen, Skogs- och Lantbruksakademiens stipendiestiftelser, Senator Emil Possehls stipendiefond, Adlerbertska Stipendiestiftelsen, Knut och Alice Wallenbergs Stiftelse, Stiftelsen Paul och Marie Berghaus donationsfond, ESF (European Science Foundation) and ACCENT (CNRS) are acknowledged for generous travel grants.

8 References

Aiken, A.C. et al., 2009. Mexico City aerosol analysis during MILAGRO using high resolution aerosol mass spectrometry at the urban supersite (T0) – Part 1: Fine particle composition and organic source apportionment. Atmos. Chem. Phys., 9(17): 6633-6653.

Arneth, A. et al., 2010. Terrestrial biogeochemical feedbacks in the climate system. Nature Geoscience, 3(8): 525-532.

Atkinson, R., 1994. Gas-phase tropospheric chemistry of organic compounds. Journal of Physical and Chemical Reference.

Atkinson, R. and Arey, J., 2003. Gas-phase tropospheric chemistry of biogenic volatile organic compounds: a review. Atmospheric Environment, 37: S197-S219.

Bell, M.L. and Davis, D.L., 2001. Reassessment of the lethal London fog of 1952: Novel indicators of acute and chronic consequences of acute exposure to air pollution. Environmental Health Perspectives, 109: 389-394.

Bernard, F. et al., 2012. Thresholds of secondary organic aerosol formation by ozonolysis of monoterpenes measured in a laminar flow aerosol reactor. Journal of Aerosol Science, 43(1): 14-30.

Bohn, B., et al., 2005. Actinometric measurements of NO_2 photolysis frequencies in the atmosphere simulation chamber SAPHIR. Atmos. Chem. Phys., 5(2): 493-503.

Brown, S.S. and Stutz, J., 2012. Nighttime radical observations and chemistry. Chemical Society Reviews, 41(19): 6405-6447.

Cengel, Y. A. 1997 Introduction to Thermodynamic and Heat Transfer, McGraw-Hill Higher Education

Cappa, C.D.C.C.D. and Wilson, K.R., 2011. Evolution of organic aerosol mass spectra upon heating: implications for OA phase and partitioning behavior. Atmospheric Chemistry and Physics, 11(5): 1895-1911.

Cocker, D.R., et al., 2001. The effect of water on gas-particle partitioning of secondary organic aerosol. Part I: alpha-pinene/ozone system. Atmospheric Environment, 35(35): 6049-6072.

Cox, R.A. and Penkett, S.A., 1971. Oxidation of atmospheric SO_2 by products of ozoneolefin reaction. Nature, 230(5292): 321-322.

de Gouw, J. and Jimenez, J.L., 2009. Organic Aerosols in the Earth's Atmosphere. Environmental Science & Technology, 43(20): 7614-7618.

de Gouw, J.A. et al., 2008. Sources of particulate matter in the northeastern United States in summer: 1. Direct emissions and secondary formation of organic matter in urban plumes. Journal of Geophysical Research-Atmospheres, 113(D8).

de Gouw, J.A. et al., 2005. Budget of organic carbon in a polluted atmosphere: Results from the New England Air Quality Study in 2002. Journal of Geophysical Research-Atmospheres, 110(D16).

DeCarlo, P.F. et al., 2006. Field-deployable, high-resolution, time-of-flight aerosol mass spectrometer. Analytical Chemistry, 78(24): 8281-8289.

Docherty, K.S., et al., 2005. Contributions of organic peroxides to secondary aerosol formed from reactions of monoterpenes with O-3. Environmental Science & Technology, 39(11): 4049-4059.

Donahue, N.M., et al., 2006. Coupled partitioning, dilution, and chemical aging of semivolatile organics. Environmental Science & Technology, 40(8): 2635-2643.

Donahue, N.M. et al., 2012. Aging of biogenic secondary organic aerosol via gas-phase OH radical reactions. Proceedings of the National Academy of Sciences of the United States of America, 109(34): 13503-13508.

Drozd, G.T. and Donahue, N.M., 2011. Pressure Dependence of Stabilized Criegee Intermediate Formation from a Sequence of Alkenes. Journal of Physical Chemistry A, 115(17): 4381-4387.

Emanuelsson, E.U. et al., 2012. Formation of anthropogenic secondary organic aerosol (SOA) and its influence on biogenic SOA properties. Atmos. Chem. Phys. Discuss., 12(8): 20311-20350.

Ervens, B., et al., 2011. Secondary organic aerosol formation in cloud droplets and aqueous particles (aqSOA): A review of laboratory, field and model studies. Atmospheric Chemistry and Physics, 11(21): 11069-11102.

Finlayson-Pitts, B.J. and Pitts, J.N., 2000. Chemistry of the Upper and Lower Atmosphere. Academic Press.

Fushimi, A. et al., 2011. Radiocarbon ((14)C) Diurnal Variations in Fine Particles at Sites Downwind from Tokyo, Japan in Summer. Environmental Science & Technology, 45(16): 6784-6792.

Ghirardo, A. et al., 2010. Determination of de novo and pool emissions of terpenes from four common boreal/alpine trees by 13CO(2) labelling and PTR-MS analysis. Plant Cell and Environment, 33(5): 781-792.

Goldstein, A.H. and Galbally, I.E., 2007. Known and unexplored organic constituents in the Earth's atmosphere. Environmental Science & Technology, 41(5): 1514-1521.

Hakola, H., et al., 2012. In situ measurements of volatile organic compounds in a boreal forest. Atmos. Chem. Phys., 12(23): 11665-11678.

Hallquist, M. et al., 2009. The formation, properties and impact of secondary organic aerosol: current and emerging issues. Atmospheric Chemistry and Physics, 9(14): 5155-5236.

Hari, P. and Kulmala, L., 2008. Boreal Forest and Climate Change. Springer Netherland, Berlin.

Heal, M.R., et al., 2012. Particles, air quality, policy and health. Chemical Society Reviews, 41(19): 6606-6630.

Heald, C.L. et al., 2010. A simplified description of the evolution of organic aerosol composition in the atmosphere. Geophysical Research Letters, 37.

Hellén, H., et al., 2008. Influence of residential wood combustion on local air quality. Science of the Total Environment, 393(2-3): 283-290.

Hill, A.V., 1913. The combinations of haemoglobin with oxygen and with carbon monoxide. I. Biochemical Journal, 7(5): 471-480.

Hinds, W.C., 1999. Aerosol Technology - Properties, Behaviour and Measurement of Airborne Particles 2nd revised edition, Wiley, New York, UK.

IPCC, 2007. Interngovernmental Panel on Climate Change: Climate Change 2007: The Physical Science Basis, Cambridge University Press, UK, 2007.

Jenkin, M.E., 2004. Modelling the formation and composition of secondary organic aerosol from alpha- and beta-pinene ozonolysis using MCM v3. Atmospheric Chemistry and Physics, 4: 1741-1757.
Jimenez, J.L. et al., 2009. Evolution of Organic Aerosols in the Atmosphere. Science, 326(5959): 1525-1529.
Johnson, D. and Marston, G., 2008. The gas-phase ozonolysis of unsaturated volatile organic compounds in the troposphere. Chemical Society Reviews, 37(4): 699-716.
Jonsson, Å.M., et al., 2008a. The effect of temperature and water on secondary organic aerosol formation from ozonolysis of limonene, Delta(3)-carene and alpha-pinene. Atmospheric Chemistry and Physics, 8(21): 6541-6549.
Jonsson, Å.M., et al., 2008b. Influence of OH scavenger on the water effect on secondary organic aerosol formation from ozonolysis of limonene, Delta(3)-carene, and alpha-pinene. Environmental Science & Technology, 42(16): 5938-5944.
Jonsson, Å.M., et al., 2006. Impact of Humidity on the Ozone Initiated Oxidation of Limonene, D3-Carene, and a-Pinene. Environmental Science and Technology, 40(1): 188-194.
Jonsson, Å.M., et al., 2007. Volatility of secondary organic aerosols from the ozone initiated oxidation of [alpha]-pinene and limonene. Journal of Aerosol Science, 38(8): 843-852.
Kanakidou, M. et al., 2005. Organic aerosol and global climate modelling: a review. Atmospheric Chemistry and Physics, 5: 1053-1123.
Koop, T., et al., 2011. Glass transition and phase state of organic compounds: dependency on molecular properties and implications for secondary organic aerosols in the atmosphere. Physical Chemistry Chemical Physics, 13(43): 19238-19255.
Kroll, J.H. et al., 2011. Carbon oxidation state as a metric for describing the chemistry of atmospheric organic aerosol. Nature Chemistry, 3(2): 133-139.
Kroll, J.H. and Seinfeld, J.H., 2008. Chemistry of secondary organic aerosol: Formation and evolution of low-volatility organics in the atmosphere. Atmospheric Environment, 42(16): 3593-3624.
Liu, B.Y.H. and Pui, D.Y.H., 1974. Submicron aerosol standard and primary, absolute calibration of condensation nuclei counter. Journal of Colloid and Interface Science, 47(1): 155-171.
Maksymiuk, C.S., et al., 2009. Secondary organic aerosol formation from multiphase oxidation of limonene by ozone: mechanistic constraints via two-dimensional heteronuclear NMR spectroscopy. Physical Chemistry Chemical Physics, 11(36): 7810-7818.
Mauldin III, R.L. et al., 2012. A new atmospherically relevant oxidant of sulphur dioxide. Nature, 488(7410): 193-196.
McMurry, P.H., 2000. A review of atmospheric aerosol measurements. Atmospheric Environment, 34(12-14): 1959-1999.
Mentel, Th. F. et al., 2009. Photochemical production of aerosols from real plant emissions. Atmospheric Chemistry and Physics, 9(13): 4387-4406.
Middleton, J. T., et al., 1950. Injury to Herbaceous Plants by Smog or Air Pollution. U.S.D.A. Plant Diss. Rep., 34, 245-525.
Molina, M.J. and Molina, L.T., 2004. Megacities and atmospheric pollution. Journal of the Air & Waste Management Association, 54(6): 644-680.

Nel, A., 2005. Air pollution-related illness: Effects of particles. Science, 308(5723): 804-806.

Nguyen, T.L., et al., 2009. Theoretical study of the gas-phase ozonolysis of beta-pinene (C10H16). Physical Chemistry Chemical Physics, 11(27): 5643-5656.

Odum, J.R. et al., 1996. Gas/particle partitioning and secondary organic aerosol yields. Environmental Science & Technology, 30(8): 2580-2585.

Olofson, K.F.G. et al., 2009. Urban aerosol evolution and particle formation during wintertime temperature inversions. Atmospheric Environment, 43(2): 340-346.

Pankow, J.F., 1994. An absorption model of gas/particle partitioning of organic compounds in the atmosphere. Atmospheric Environment, 28(2): 185-8.

Pankow, J.F. and Asher, W.E., 2008. SIMPOL.1: a simple group contribution method for predicting vapor pressures and enthalpies of vaporization of multifunctional organic compounds. Atmos. Chem. Phys., 8(10): 2773-2796.

Pathak, R.K. et al., 2012. Influence of Ozone and Radical Chemistry on Limonene Organic Aerosol Production and Thermal Characteristics. Environmental Science & Technology, 46(21): 11660-11669.

Pathak, R., et al., 2008. Ozonolysis of beta-pinene: Temperature dependence of secondary organic aerosol mass fraction. Environmental Science & Technology, 42(14): 5081-5086.

Rader, D.J., et al.,1987. Evaporation rates of monodisperse organic aerosols in the 0.02- to 0.2-mm-diameter range. Aerosol Science and Technology, 6(3): 247-60.

Renbaum, L.H. and Smith, G.D., 2011. Artifacts in measuring aerosol uptake kinetics: the roles of time, concentration and adsorption. Atmospheric Chemistry and Physics, 11(14): 6881-6893.

Riipinen, I., et al., 2010. Equilibration time scales of organic aerosol inside thermodenuders: Evaporation kinetics versus thermodynamics. Atmospheric Environment, 44(5): 597-607.

Rohrer, F. et al., 2005. Characterisation of the photolytic HONO-source in the atmosphere simulation chamber SAPHIR. Atmospheric Chemistry and Physics, 5: 2189-2201.

Saathoff, H. et al., 2009. Temperature dependence of yields of secondary organic aerosols from the ozonolysis of alpha-pinene and limonene. Atmospheric Chemistry and Physics, 9(5): 1551-1577.

Salo, K., et al., 2010. Aerosol Volatility and Enthalpy of Sublimation of Carboxylic Acids. Journal of Physical Chemistry A, 114(13): 4586-4594.

Salo, K. et al., 2011a. Volatility of secondary organic aerosol during OH radical induced ageing. Atmospheric Chemistry and Physics, 11(21): 11055-11067.

Salo, K. et al., 2011b. Thermal Characterization of Aminium Nitrate Nanoparticles. Journal of Physical Chemistry A, 115(42): 11671-11677.

Saukko, E. et al., 2012. Humidity-dependent phase state of SOA particles from biogenic and anthropogenic precursors. Atmos. Chem. Phys., 12(16): 7517-7529.

Seinfeld, J.H. and Pandis, S.N., 2006. Atmospheric Chemistry and Physics: From Air Pollution to Climate Change, Wiley ISBN: 978-0-471-72018-8

Spracklen, D.V. et al., 2008. Contribution of particle formation to global cloud condensation nuclei concentrations. Geophysical Research Letters, 35(6).

Spracklen, D.V. et al., 2011. Aerosol mass spectrometer constraint on the global secondary organic aerosol budget. Atmos. Chem. Phys., 11(23): 12109-12136.

Steinbrecher, R. et al., 2000. Biogenic and anthropogenic fluxes of non-methane hydrocarbons over an urban-impacted forest, Frankfurter Stadtwald, Germany. Atmospheric Environment, 34(22): 3779-3788.

Stull, R. B., 1988. An Introduction to Boundary Layer Meteorology. Kluwer Academic Publishers.

Tillmann, R. et al., 2010. Influence of relative humidity and temperature on the production of pinonaldehyde and OH radicals from the ozonolysis of alpha-pinene. Atmospheric Chemistry and Physics, 10(15): 7057-7072.

Tobias, H.J. and Ziemann, P.J., 2001. Kinetics of the gas-phase reactions of alcohols, aldehydes, carboxylic acids, and water with the C13 stabilized Criegee intermediate formed from ozonolysis of 1-tetradecene. Journal of Physical Chemistry A, 105(25): 6129-6135.

Tritscher, T. et al., 2011. Volatility and hygroscopicity of aging secondary organic aerosol in a smog chamber. Atmospheric Chemistry and Physics, 11(22): 11477-11496.

Vereecken, L., et al., 2012. The reaction of Criegee intermediates with NO, RO_2, and SO_2, and their fate in the atmosphere. Physical Chemistry Chemical Physics, 14(42): 14682-14695.

Vesterinen, M., et al., 2007. Effect of particle phase oligomer formation on aerosol growth. Atmospheric Environment, 41(8): 1768-1776.

Vingarzan, R., 2004. A review of surface ozone background levels and trends. Atmospheric Environment, 38(21): 3431-3442.

Virtanen, A. et al., 2010. An amorphous solid state of biogenic secondary organic aerosol particles. Nature, 467(7317): 824-827.

Virtanen, A. et al., 2011. Bounce behavior of freshly nucleated biogenic secondary organic aerosol particles. Atmospheric Chemistry and Physics, 11(16): 8759-8766.

Wang, S.C. and Flagan, R.C., 1990. Scanning Electrical Mobility Spectrometer. Aerosol Science and Technology, 13(2): 230-240.

Wang, Y. et al., 2007. Arabidopsis EIN2 modulates stress response through abscisic acid response pathway. Plant Molecular Biology, 64(6): 633-644.

Whitby, K. T. and Sverdrup G. M. 1980. California Aerosols: Their Physical and Chemical Characteristics. Advances in Environmental Science and Technology 8, 477-525

Wielicki, B.A., et al., 1995. Mission to planet earth - role of clouds and radiation in climate. Bulletin of the American Meteorological Society, 76(11): 2125-2153.

Winklmayr, W. et al., 1991. A new electromobility spectrometer for the measurement of aerosol size distributions in the size range from 1 to 1000 nm. Journal of Aerosol Science, 22(3): 289-296.

Winterhalter, R. et al., 1999. Products and mechanism of the gas phase reaction of ozone with beta-pinene. Journal of Atmospheric Chemistry, 35(2): 165-197.

Zhang, D. and Zhang, R., 2005. Ozonolysis of alpha-pinene and beta-pinene: Kinetics and mechanism. Journal of Chemical Physics, 122(11).

Zhang, Q. et al., 2007. Ubiquity and dominance of oxygenated species in organic aerosols in anthropogenically-influenced Northern Hemisphere midlatitudes. Geophysical Research Letters, 34(13).

Zobrist, B., et al., 2008. Do atmospheric aerosols form glasses? Atmos. Chem. Phys., 8(17): 5221-5244.

ISBN 978-91-628-8620-2
Printed by Ale Tryckteam AB